SMHI RO
Nr 10, January 1990

SEA ICE PROPERTIES STUDIED FROM THE ICEBREAKER TOR DURING BEPERS -88

by

Fransson L. Håkansson B. Omstedt A. and Stehn L.

Front page:

The research team at the icebreaker TOR from left and first line
Paula Kankanpää and Caren Garrity
second line
Lars Åström, Ken Asmus, Mats Moberg, Thomas Thompson, Barbara Burns,
Anders Omstedt, Björn Larsson and Anders Gustavsson
third line
Bertil Håkansson, Lars Stehn, Sver Riger, Volkmar Wisman and Bertil Brusmark

SMHIs Tryckeri Norrköping 1990

SMHI REPORTS OCEANOGRAPHY Nr 10, January 1990

SEA ICE PROPERTIES STUDIED FROM THE ICEBREAKER TOR DURING BEPERS -88

by

Fransson[1], L., Håkansson[2], B., Omstedt[2], A., and Stehn[1], L.

[1]Luleå University of Technology, S-951 87 LULEÅ, Sweden
[2]The Swedish Meteorological and Hydrological Institute,
S-60176 NORRKÖPING, Sweden

Issuing Agency
SMHI
S-601 76 NORRKÖPING
SWEDEN

Report number
RO No 10

Report date
January 1990

Author (s)
Fransson L, Håkansson B, Omstedt A, Stehn L

Title (and Subtitle)
Sea ice properties studied from the icebreaker TOR during BEPERS-88.

Abstract
The report presents sea ice data taken during BEPERS-88 experiment in the Bothnian Bay. Several physical properties are presented and analysed. In general the data illustrate that sea ice is a most complex medium with horizontal and vertical variations. Any analysis of remotely sensed data must therefore carefully consider the ground truth data.

Key words
Sea ice, Properties, Baltic Sea

Supplementary notes

Number of pages
20

Language
English

ISSN and title
0283-1112 SMHI Reports Oceanography

Report available from:
SMHI
S-601 76 NORRKÖPING
SWEDEN

LIST OF CONTENTS

ABSTRACT

The report presents sea ice data taken during the BEPERS-88 experiment in the Bothnian Bay. Several physical properties (crystal structure, salinity, temperature, density, porosity, and strength) are presented and analysed. In general the data illustrate that sea ice is a most komplex medium with horizontal and vertical variations. Any analysis of remotely sensed data must therefore carefully consider the ground truth data.

1. INTRODUCTION

The present investigation of the sea ice variables measured in the southern part of the Bothnian Bay in the Baltic Sea (see Figure 1) was one of the contributions to the ground measurement programme during the field experiment BEPERS-88 (Bothnian Experiment in Preparation for ERS-1); see also Fransson et al. (1989). The experiment objectives were mainly to test and analyse remotely sensed image data from a synthetic aperture radar (SAR) and to evaluate the ability of SAR for operational sea ice mapping in the Baltic. In this context the ice core data and other field measurements are of great importance. It is also believed that the present set of data is of general interest for the understanding of sea ice physics in brackish coastal seas.

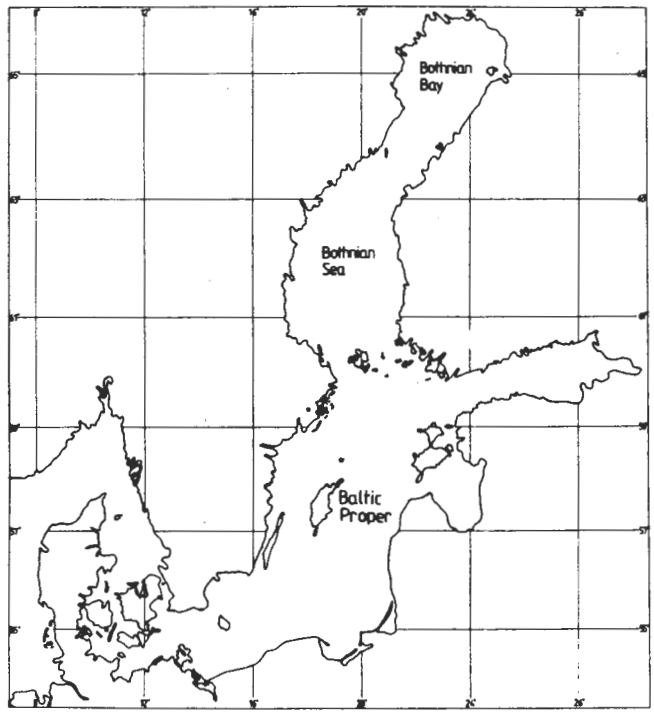

Figure 1. Overview of the Baltic area.

Earlier studies of sea ice properties in the Bothnian Bay have been reported by Palosuo (1961), Fransson (1983), Omstedt (1985), and Leppäranta (1987). The works by Palosuo (1961) and Fransson (1983) were performed from the inner skerries, while the works by Omstedt (1985) and Leppäranta (1987) were performed in the open sea. For example, the crystal structure observations presented by Leppäranta (1987) were sampled during the mid-winter of 1985 and illustrated that the ice structure was mainly due to Columnar Ice. This is in contrast to the measurement by Omstedt (1985) from the mid-winter of 1984, when Granular Ice (due to Snow Ice and Frazil Ice), Columnar Ice and Mixed Ice were frequently observed. These results illustrate that different sites and different years may give different ice signatures with respect to the vertical ice crystal structure.

The ice formation in the Bothnian Bay skerries started normally during the winter of 1987/88 despite the mild weather, which caused delayed ice formation in the open sea. The whole bay was not ice-covered until late January, although new ice covered the bay occasionally before this time; leads and cracks were present during the whole winter. In the end of April the ice cover finally broke up during fresh northerly winds. The time evolution of a few meteorological parameters is illustrated in Figure 2 a, where wind, air temperature, mean cloudiness and relative humidity are shown. Figure 2 b illustrates the cumulative number of freezing days during this winter. According to empirical relationships between this parameter and ice thickness (e.g. Maykut, 1986) the level ice thickness during March 1988 was approximately 30 to 40 cm. This was also the typical range of level ice thickness observed in the investigation area. The daily observations of air temperature and cloudiness made during the BEPERS-88 are shown in Figure 2 c. For example, almost cloudless conditions occurred only on March 9, when the aerial photography was made. The meteorological observations were made at the synoptic weather station of Holmögadd located in the western part of Norra Kvarken.

The sea ice properties measured during March 3 and 9, 1988, included density, salinity, temperature, pressure, and crystal structure. The methods and procedures involved are described in the following section, whereafter the results are presented in Section 3. Finally, a discussion concerning the spatial distribution of the parameters follows.

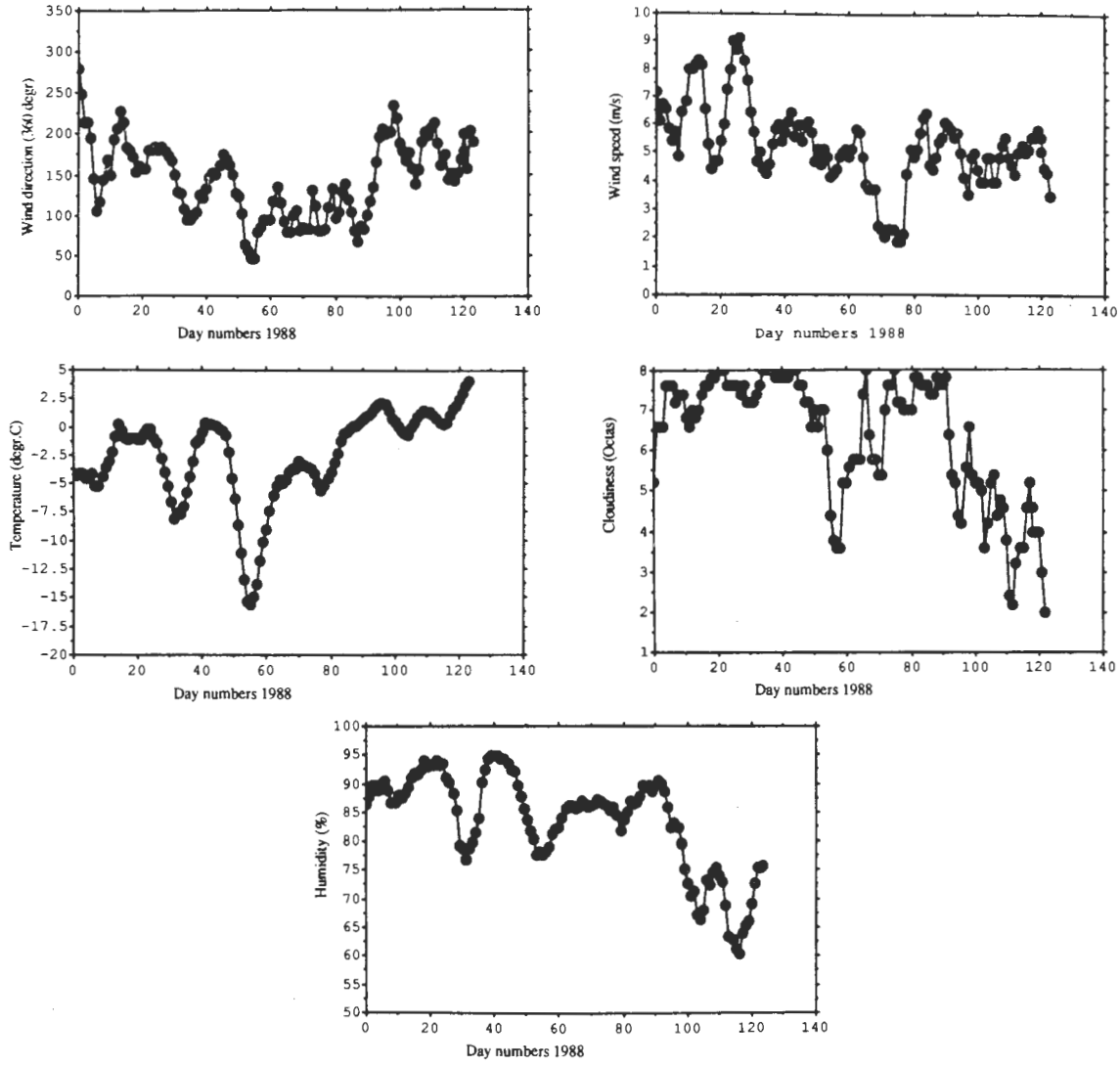

Figure 2 a. Observations of cloudiness, humidity, temperature, wind speed and direction during January to May at the Holmögadd weather station. The presented data are smoothed using the running mean technique over a 7 day period.

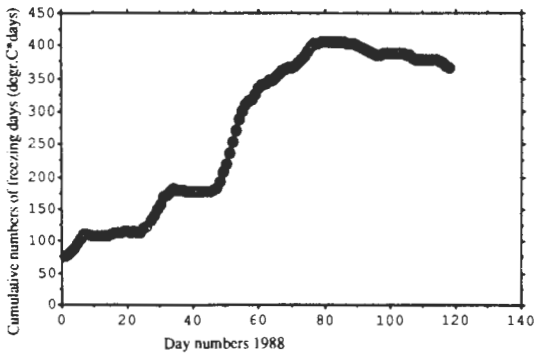

Figure 2 b. The cumulative number of freezing days, using the smoothed temperature observations shown in Figure 2 a.

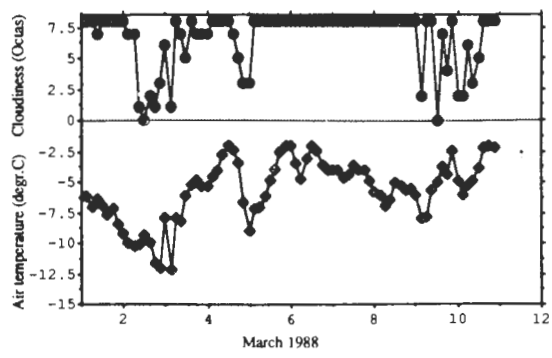

Figure 2 c. Observations from Holmögadd made every 3 hour, during the BEPERS-88 experiment.

2. TEST METHODS AND PROCEDURES

2.1 Area of data sampling

The investigation area was selected so that different types of ice morphology were covered and that the areal extent of these was large enough to be identified in the images. In the field experiment a relative coordinate system was used, which consisted of deployed markers as radar reflectors, tarpaulins, and flags. The measured positions in this coordinate system was estimated with an accuracy of a few meters by using the DECCA navigation system and simply by taking the bearing and distance to the marked points from the icebreaker Tor. The final size of the investigation area was selected to be 1 x 2 km with ice core sampling taken around the periphery. The distance between the sampling positions was roughly 500 m. Additional cores were taken in collaboration with other field measurements.

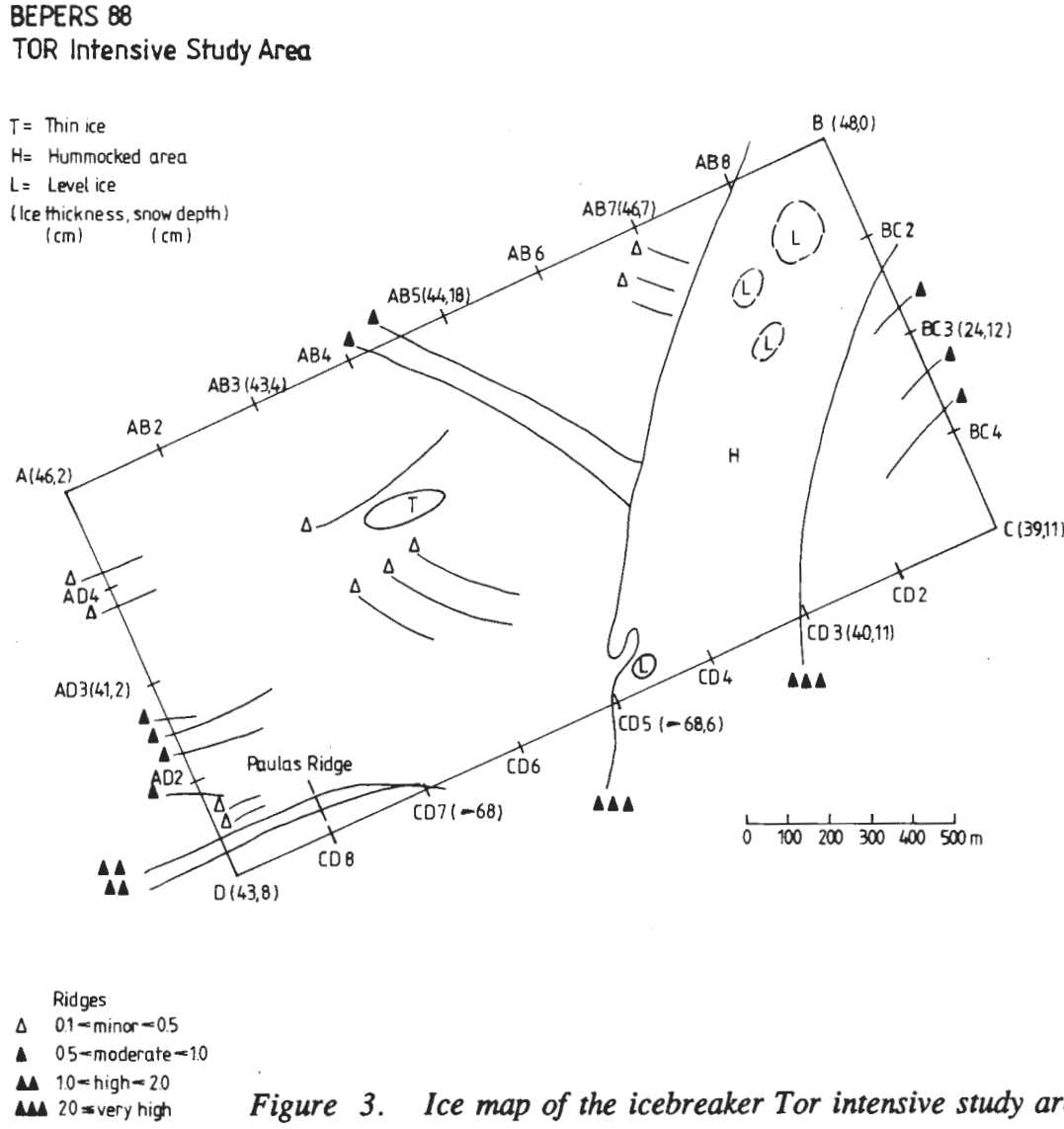

Figure 3. Ice map of the icebreaker Tor intensive study area.

The study area is schematically shown in Figure 3, in which also the main ice morphology is illustrated. The southwestern part of the area consists mainly of level ice crossed by minor to moderate ice ridges. In the northeastern part a shear ridge area, approximately 350 meters wide, was present, including a gliding ice zone on the eastern side. Ice blocks with heights above two meters were common in the area. An aerial photography from the studied area is shown in Figure 4. Note also the shear or gliding zone in the eastern part of the shear ridge area, as well as the spatial variability in snow extent and orientation of the snow patches. According to observations from level ice in the southwestern part of the area the mean snow depth was 0.12 m with a r.m.s. deviation of 0.26 m. Snow and ice depth were also recorded where ice cores were sampled; these data are included in Figure 3.

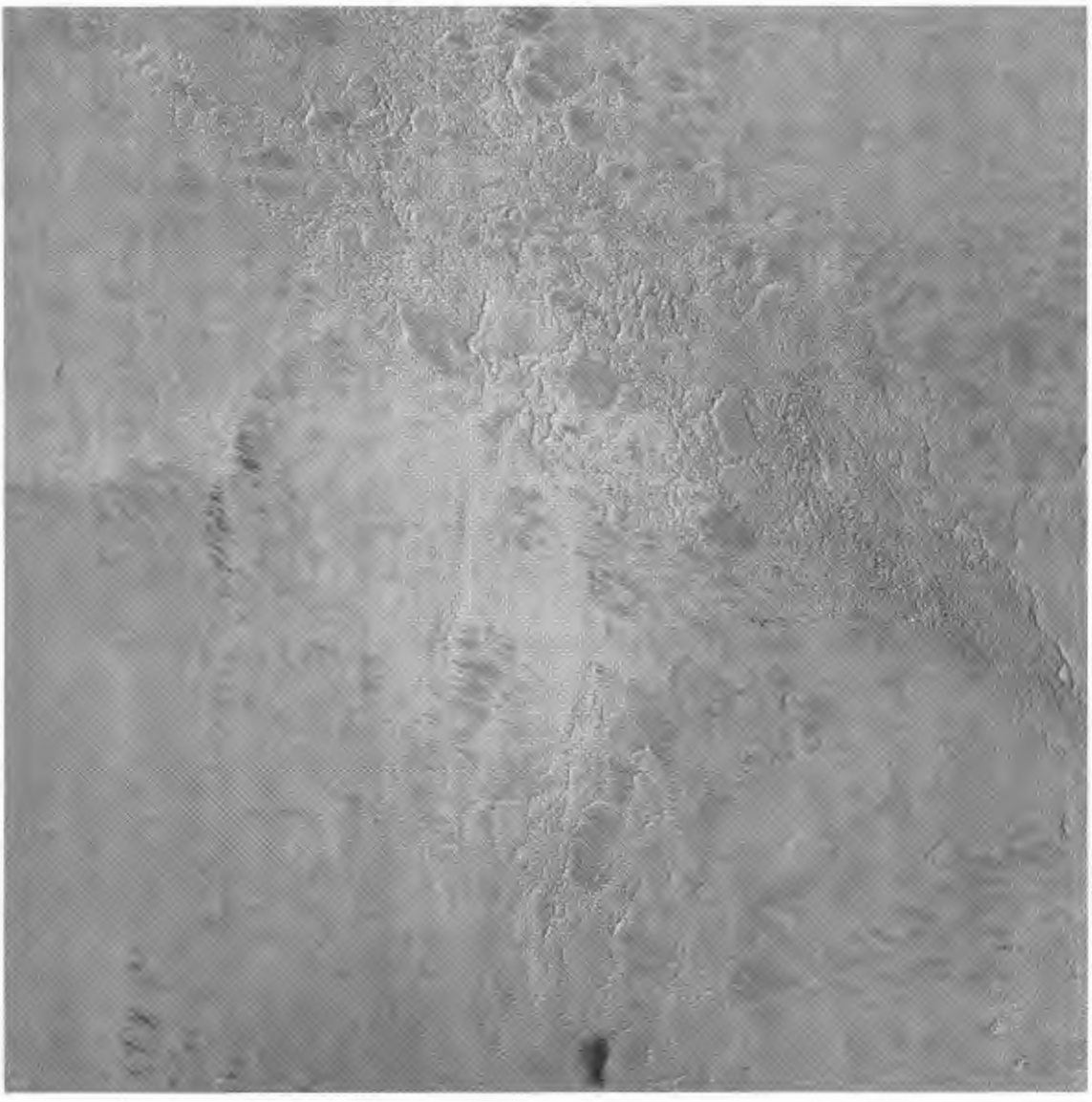

Figure 4. Aerial photography of Tor intensive study area.

2.2 Instruments and methods for ice core measurements

The cores were sampled in the ice with a driller of radius 0.20 m mounted on a motor-driven apparatus. This made the sampling procedure quick, and thus allowed several cores from the same station to be taken. Salinity and density samples along with temperature were always taken from the same core.

The in situ temperature was recorded at the standard depths of 0.05, 0.15, 0.25, 0.35, 0.45, and 0.55 m from the ice surface. This was done in an extra drilled hole almost reaching to the bottom of the ice. The measurements were made with a Keithley 871 digital thermometer with the resolution of 0.1 °C. At the outdoor ice laboratory on board the icebreaker Tor, the ice core temperature was again recorded before salinity and density samples were taken. The salinity samples were melted and stored for analysis at the SMHI laboratory in Norrköping. This was done on the Hummon and Brown inductive coupled salinity instrument with an accuracy of 0.02 units. The density estimates were made by using the volume and weight method. Samples were collected with 0.10 m intervals by drilling, in the horizontal direction, pieces from the original ice core. The volume of these pieces was estimated from the volume formula of a perfect cylinder:

$$V = \pi\, d^2\, l\, /\, 4 \qquad (2.2.1)$$

where d and l are the diameter and length of the cylinder, respectively. The length scales were measured with an accuracy of 0.001 m. The mass (M) of the cylinder was measured on the Mettler digital balance with an accuracy of 0.0001 kg. The density estimate of the sample then follows from the expression:

$$\rho = 4\, M\, /\, \pi\, d^2\, l \qquad (2.2.2)$$

The accuracy of the density estimates may be found by using the formula for the maximum error, yielding:

$$\Delta\rho\, /\, \rho = \Delta M\, /\, M + 2\, \Delta d\, /\, d + \Delta l\, /\, l \qquad (2.2.3)$$

Typical values of M, d, and l were 0.500 kg, 0.070 m, and 0.150 m, respectively. The relative accuracy according to equation (2.2.3) is ± 0.004, and the absolute accuracy is ± 3.5 kg/m^3. It may be noted that the first and third terms on the right hand side of equation (2.2.3) are O(10^{-4}), while the second therm (cylinder diameter) is almost O(10^{-3}).

2.3 Ice strength testing

The principle of the pressure meter is very simple. The probe made of tubular rubber membrane is filled with liquid (here anti-freeze) and expanded. If the probe is placed in a borehole in the ice, the expansion is restricted by the ice. The probe deforms the ice and, if the pressure is high enough, the ice crushes. Because of the large volume of ice in the ice sheet there is no complete failure, only a volume around the probe cracks. To prevent the probe from blasting, only a limited volume is allowed, sometimes less than needed to plastify the ice completely. It is also important to keep the rate of deformation constant when making field tests, since the ice strength is rate-dependent. This is partly the case if a constant rate of volume is used when filling the probe. The pumping tempo is therefore controlled with an electronic buzzer. The pressure of the liquid is registered by a manometer and the volume by measuring the height in a tube connected to the reservoir. The pressure meter is shown in Figure 5.

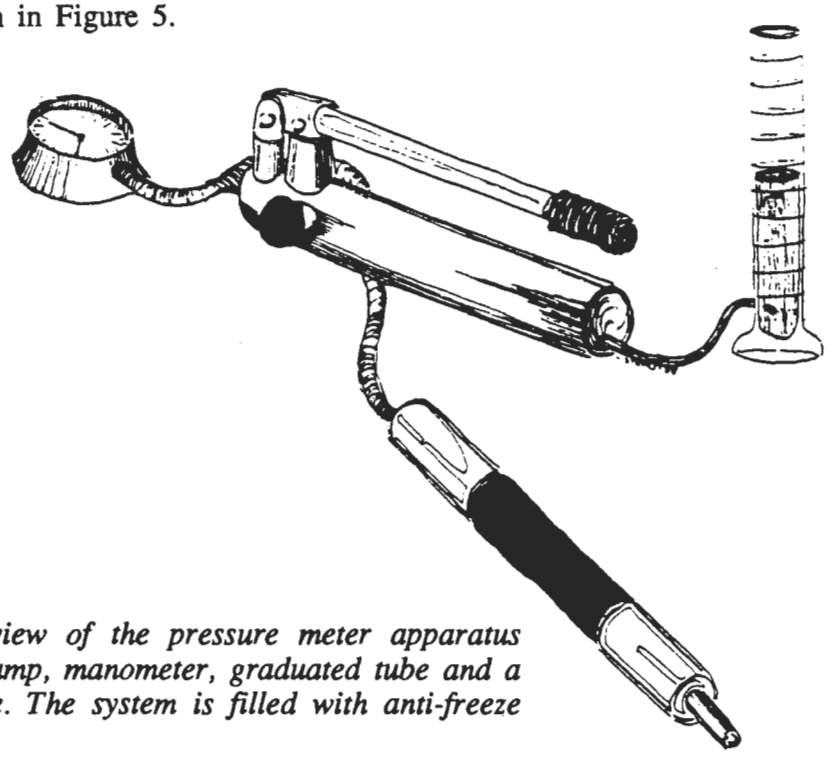

Figure 5. Schematic view of the pressure meter apparatus including pump, manometer, graduated tube and a flexible pipe. The system is filled with anti-freeze liquid.

The evaluation of the crushing strength from the pressure meter data can be made by assuming that the peak pressure during a run correlates with the uniaxial compressive strength. This is obtained from small horizontal samples taken close to the pressure meter boreholes. Strain rate and temperature should be kept as close to the field testing conditions as possible. The assumption made by Michel and Hodgson (1982) was that the correlation could be written:

$$\sigma_c = p_y / c_i \qquad (2.3.1)$$

Here σ_c is the crushing strength, P_y the yield pressure from the pressure meter tests and c_i a constant for each ice type. Values on the constant c_i were found by Michel and Hodgson for freshwater ice close to the melting point; these are shown in Table 2.3.

Tabell 2.3. The correlation constant c_i for freshwater ice at 0 °C.

Type of ice	Pressure meter yield strength (MPa)	Crushing* strength (MPa)	c_i
S2	12.0 ± 1.0	3.0	4
S1	14.1 ± 1.0	4.7	3
T1	5.6 ± 2.3	2.3	2.5
T3	12.8 ± 1.6	4.2	3

* The laboratory tests were done at another temperature than the pressure meter test and corrected (somewhat arbitrary) to the field temperature.

The properties of the low salinity sea ice close to the lighthouse of Nordströmsgrund have been examined by the Luleå University of Technology during a three-year period 3 to 5 times a year (Danielsson et al., 1988). At two occasions also pressure meter tests were carried out. Ice thickness, temperature, density, strength were determined at each 10 cm of the sheet. The average strength was compared

to the yield stress obtained from an average curve of six pressure meter tests. The total pressure was reduced by a seating pressure corresponding to the membrane resistance. From these two tests the constant c_i was determined as 4.4 and 4.5 respectively. These values are in good agreement with the findings of Michel and Hodgson (1982), who suggested $c_i = 4$ for S2-ice.

2.4 Crystal structure analysis

The ice crystal structures were investigated in a similar manner as those presented by Omstedt (1985). Vertical thin sections from the ice cores were prepared on board the icebreaker Tor. The ice specimens were then put on a polarizing table, where photographs were taken.

3. RESULTS

In the present section some results are briefly shown; all basic data, however, are presented in Attachments A to C. The classification of ice crystal structure, photos of the crystal structure including positions and the temperature, salinity, and density along with calculations of porosity are presented in Attachments A, B, and C, respectively.

3.1 Crystal structure

Several classification schemes on ice crystal structure are available today (e.g. Michel, 1978, and Cox et al., 1984), but they all seem to be rather unsatisfactory to use. The complex crystal structure in sea ice with multi-layered ice of different origins causes several problems in determining crystal type. For example, the distinguishing between Snow Ice and Frazil Ice can be difficult due to rafting and ridging. Hence, in the present work only Granular Ice (which can either be of snow or ice origin) and Columnar Ice are distinguished.

Figure 6 shows one example of the vertical structure found at station AB7. Two layers of Columnar Ice appears, separated by a layer of Granular Ice. The vertical structure indicates that the ice has been rafted.

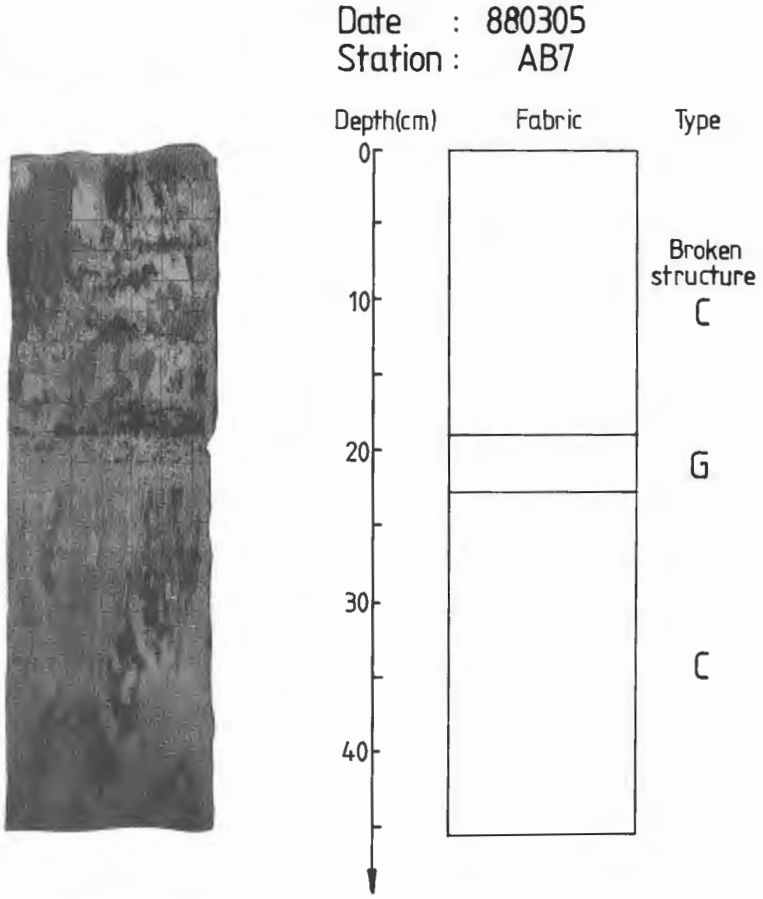

Figure 6. Thin section showing ice crystal structure.

3.2 Salinity and density

The horizontal mean and standard deviations of the salinity and density profiles are presented in Figure 7. The vertical salinity profile is C-shaped, a condition which almost all individual ice cores conform to. In the upper part of the ice the salinity varied most with surface values between 0.67 and 1.31 PSU (Practical Salinity Units), whereas the mean ice salinity was approximately one fifth of the surface water salinity.

The mean density increased towards the bottom except in those ice cores with an ice thickness larger than 0.45 m, where the density decreased again close to the bottom. The number of these thicker ice cores were only three, which may be the reason for the large standard deviation found here. At mid depths the ice density

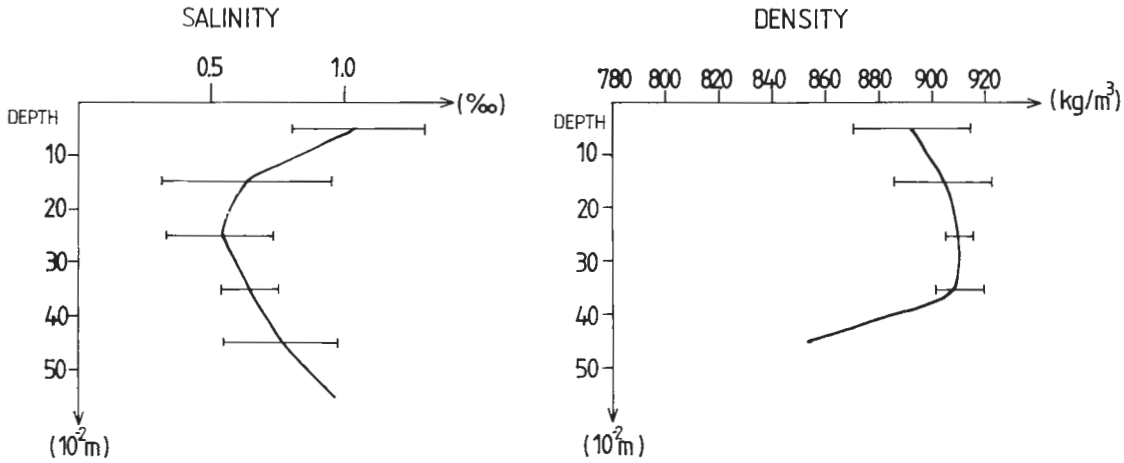

Figure 7. Mean salinity and density profiles.

was less scattered around the mean, reaching almost the estimated accuracy of the measurements. Note, however, that in the rest of the data the standard deviation for both salinity and density exceeded the accuracy of the salinity measurements and the calculated maximum error in the density estimate, respectively. Hence, the standard deviation of salinity and density indicates a dependence on physical conditions.

3.3 Temperature

The ice core in situ temperature data are horizontally averaged using ice core data sampled during a single day. The vertical profile of ice temperature for each day was almost linear with a slope of 5.0 °C/m, according to Figure 8. During this period the sea water surface temperature and salinity were -0.2 °C and 4.0 PSU respectively, which is the freezing point of sea water at this salinity.

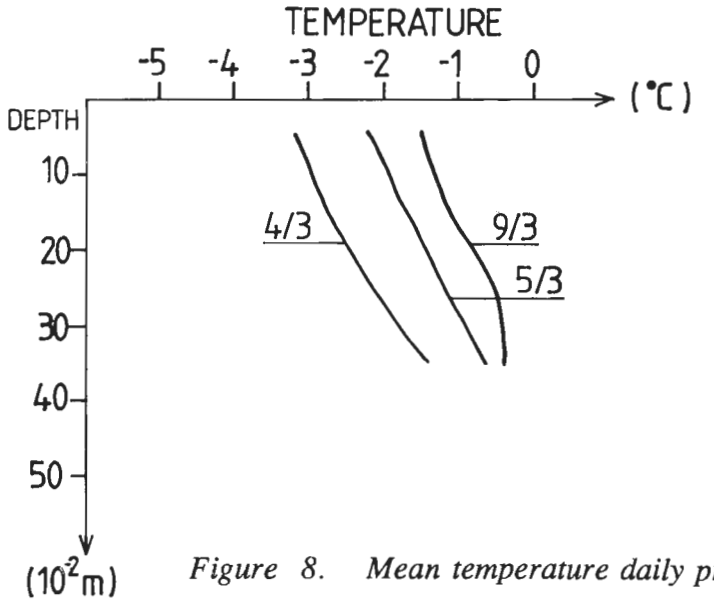

Figure 8. Mean temperature daily profiles.

3.4 Brine and gas volume

The porosity of ice is an important physical quantity, determining its mechanical, electrical and thermal properties. The porosity of sea ice involves both gas (air) and brine volumes. These are complicated to measure and only a few investigations have been done so far (e.g. Nakawo, 1983). Instead, the attention has been concentrated on methods for calculating the porosity from measurements of salinity, temperature and density (e.g. Cox and Weeks, 1983, and Schwerdtfeger, 1963).

The sea ice found in the Baltic Sea is of brackish water origin and, in some skerries with river water runoff, of fresh water origin. Hence, ice salinity may vary between zero and a few PSU. The winter climate in the area is varying with warm weather conditions occurring frequently, and sea ice temperatures just below zero are therefore not unusual. To obtain the sea ice porosity, especially at these temperatures and salinities, the method developed by Schwerdtfeger (1963) is used in the present study. This method was briefly reviewed in Håkansson and Thompson (1988) and used for porosity estimates at a site in the western part of the Bothnian Sea during the BEPERS PILOT STUDY 1987.

The equations for relative gas and brine volume were found to be:

$$\nu_a = 1 - \rho / \rho_w [\rho_w / \rho_i (1-S / 1000) - (-55.1 /\Theta) (\rho_w-\rho_i) / \rho_i (S / 1000)] \qquad (3.4.1)$$

$$\nu_b = -55.1 \rho S / (\rho_w \Theta 1000) \qquad (3.4.2)$$

Here ρ, S and Θ are the ice density (kg/m^3), salinity (PSU) and temperature ($^\circ$C), respectively. ρ_w is the water density (= 1000 kg/m^3) and ρ_i is the fresh ice density (= 917 kg/m^3), which is assumed to be temperature-independent.

The density calculations were based on measurements carried out at the ship laboratory. In general the laboratory temperature of the ice differed from the in situ temperature. Porosity estimates based on the laboratory temperature are therefore not exactly the same as those of in situ porosity. Theoretical relationship of the porosity dependence on the temperature is given by Cox and Weeks (1983). In the present investigation, however, it is assumed that this temperature dependency is negligible, and the porosity can be calculated using the in situ temperatures and densities and salinities determined in the laboratory. The horizontally mean and standard deviations of these calculations are shown in Figure 9.

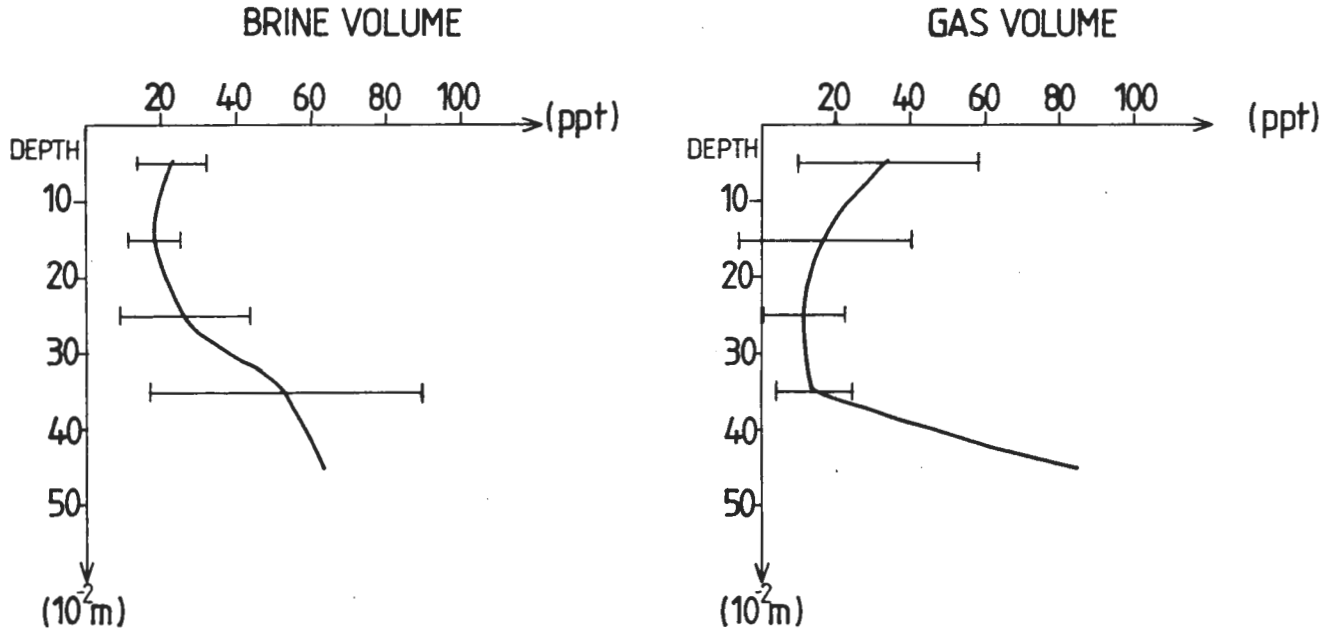

Figure 9. Mean brine and gas porosity profiles.

3.5 Strength

Pressure meter tests were carried out at each of the 10 stations in the intensive study area. The peak pressure was measured in six holes evenly spaced along a circle with a radius of about 4 m. In Table 3.5. , the average pressure from each station together with ice thickness, probe depth, and ice temperature at the actual test level are given.

Tabell 3.5. Index strength.

Station No.	Ice thickness (cm)	Probe depth (cm)	Ice temp. (C)	Peak pressure (MPa)	Index strength (MPa)
AB1	44 ± 2	23	-2.8	11.9	3.0
AB3	41 ± 1	22	-3.5	11.9	3.0
AB5	61 ± 30	15	-0.7	6.5	1.6
AB7	53 ± 1	26	-2.2	8.9	2.2
DA3	41 ± 1	20	-1.4	9.1	2.3
BC3	28 ± 0.5	12	-2.1	6.7	1.7
CD9	49 ± 1	25	-2.2	9.0	2.3
CD7	48 ± 5	22	-2.4	9.9	2.5
CD3	39 ± 1	20	-2.6	9.6	2.4
CD1	40 ± 1	20	-1.5	7.8	1.9

Mechanical tests of ice are intended to give information on the strength of the material, in this case the crushing strength. However, since the variation of the proportionality factor (c_i) of eq. (2.3.1) is not known for the ice types found during this experiment, a constant value of 4 for a similar ice type is used to correlate the measured yield pressure with the crushing strength. This estimate of the strength of the material is referred to as the index strength. To improve the knowledge of the factor c_i further it is necessary to investigate the stress field around the probe in more detail than was possible in this study.

An attempt is made to relate the variation of index strength with ice porosity and temperature. From a practical point of view, porosity is usually expressed as brine volume or even the square root of the brine volume, but strictly speaking it also includes the air volume. The air volume is negligible compared with the total porosity only for ice salinities greater than 3 to 5 PSU. In Figure 11 the index strength is plotted against brine volume and the sum of brine and gas volume, whereas in Figure 11 the index strength is plotted against temperature. These results indicate that this study does not provide enough information, which can explain the variation of index strength. Nevertheless, the general form of the curves in Figures 10 and 11 follows the trend of increasing strength with decreasing porosity and temperature observed elsewhere.

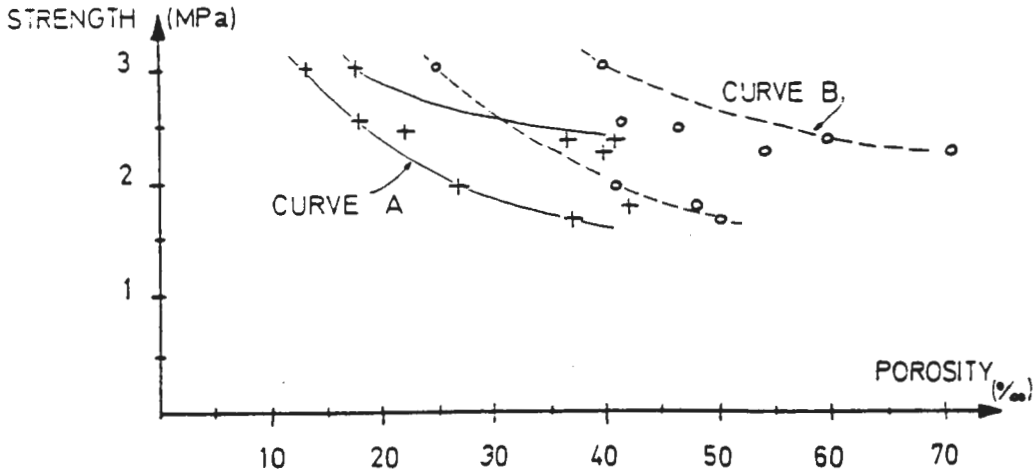

Figure 10. Variation of index strength versus porosity; for case A brine volume is used, whereas for case B the sum of brine and gas volumes is used.

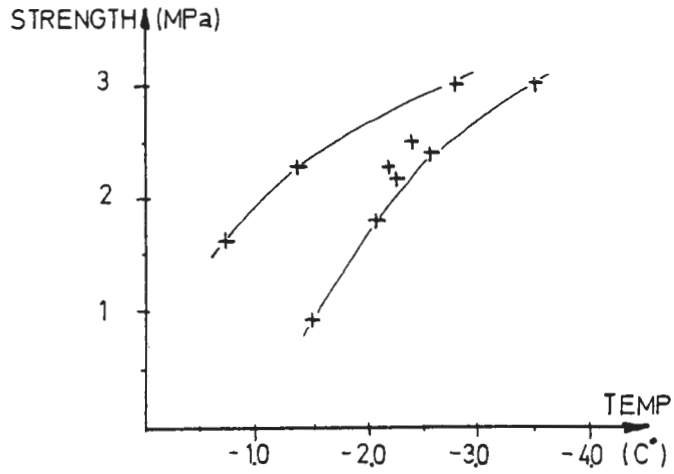

Figure 11. Variation of index strength versus temperature.

4. DISCUSSION

In the present section, an attempt is made to analyse the surface ice structure using the parameters of porosity, density, and crystal structure, so that the spatial distribution can be qualitatively described. The sum of the brine and gas volumes constitutes the porosity. The density and porosity estimates taken from 0.05 and 0.15 m below the ice surface are given in Figure 12, a and b. There is a general decrease of density with increasing porosity, although the regression analysis suggests a slightly different dependence at 0.05 and 0.15 m. This is probably due to different salinity and temperature at the two depths. A comparison of these results with crystal structure classification shows that sea ice with a density above 900 kg/m^3 and a porosity below 0.05 are of Columnar and Mixed structure, whereas ice

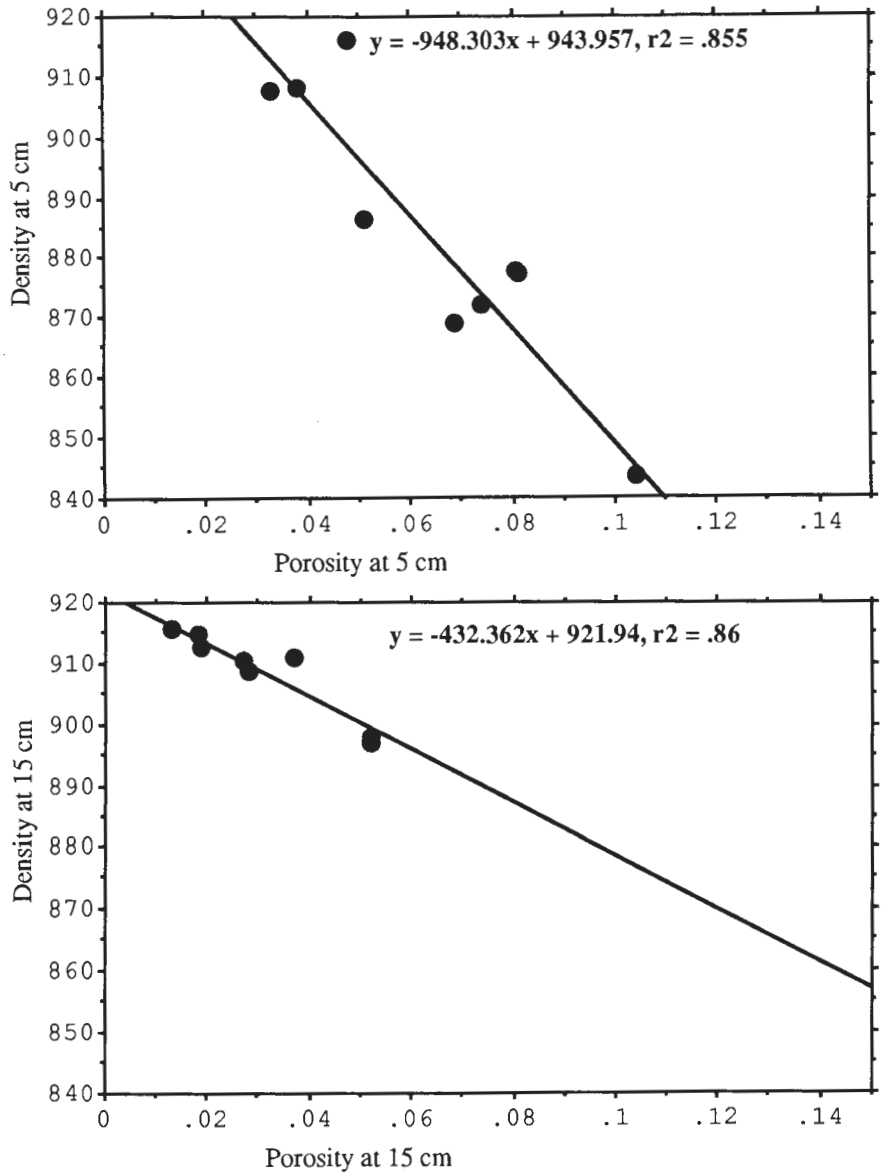

Figure 12. Variation of density and porosity at 0.05 m and 0.15 m from the sea ice surface.

with a density below 900 kg/m^3 and a porosity above 0.05 is Granular in structure. At 0.05 m both Granular, Mixed or Columnar Ice are present, but at 0.15 m Columnar and Mixed Ice dominate. Two point measurements (CD3 and CD7) have been exluded in this analysis; these are classified as Granular but have density and porosity similar to the Mixed and Columnar Ice. The reason for this is not known, but since the sea ice occured layered with many floes over each other at CD7, the surface layer is hydrostatically lifted, and this may cause the salt to be drained and the gas volumes to be refrozen. In the core from CD3 the measurements made at

0.05 m are from a zone where both Granular and Mixed Ice appears, and therefore they can not be clearly distinguished with respect to this ice structure scheme. Also the porosity at 15 cm depth at BC3 appears unrealistic, apparently due to the high temperature.

The sea ice can also be characterized using vertical averaged porosity and ice thickness. In Figure 13 the dependence between these two parameters is illustrated. Note, however, that the data from CD3, CD5, and CD7 are excluded, since the total ice depth was larger than the length of the drilling device and was therefore not properly measured. Nevertheless, the relation suggests that porosity increases with decreasing thickness. This is in agreement with the general idea that thin ice represents young ice with higher salinity and brine volumes than thick older ice.

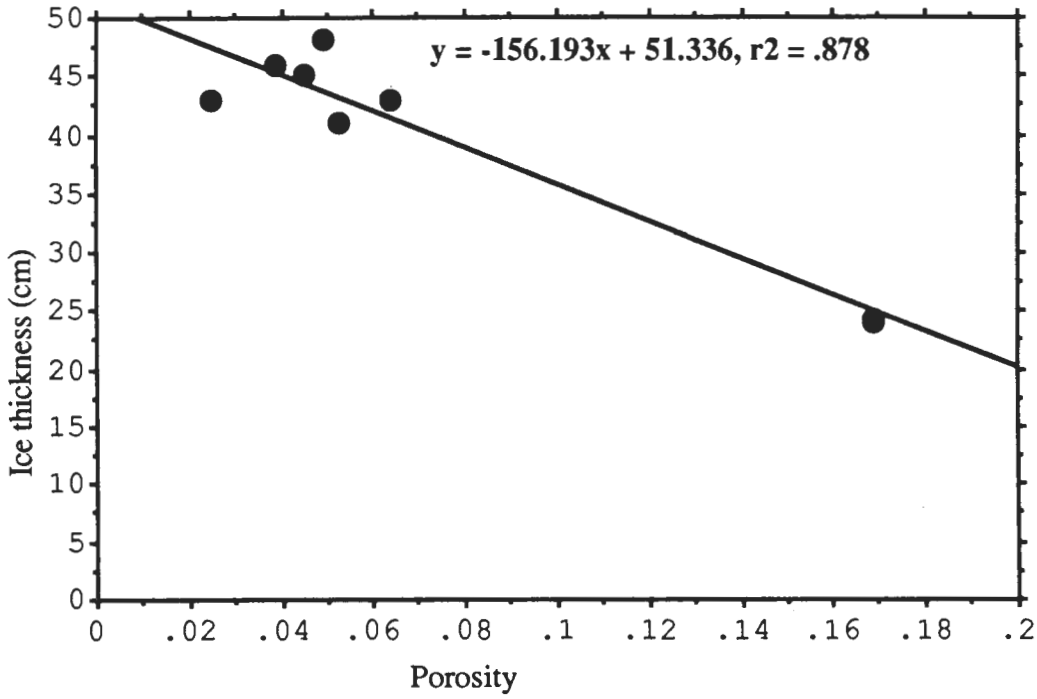

Figure 13. Variation of vertical averaged porosity and ice thickness taking all data points into account except CD7 and CD9, at which the total ice thickness was not measured due to ice floe layering.

5. SUMMARY AND CONCLUSIONS

This investigation aimed at measuring the vertical and horizontal distribution of sea ice physical properties. In general, the measuring technique produced high quality data, including both in situ and laboratory measured temperature, so that porosity

calculations can be compensated for the temperature history of the sample when salinity and density are determined at the laboratory. Especially the calculation of density was successful with an obtained relative accuracy of 0.4 %.

The mean vertical distribution of properties found in this study agrees with other measurements carried out in the Gulf of Bothnia, whereas the horizontal variations at meso scale are less known. An attempt to distinguish these at the sea ice surface in the intensive study area, on the basis of the above discussed correlation of parameters is made. In this case the northwestern part (including measurement points AB5, AB7, and AB9) contains ice of high density and low porosity which is classified as either Columnar or Mixed Ice. In the remaining area Granular Ice dominates, which contains porosities higher than 0.05 and densities lower than 900 kg/m^3.

However, the sample sites were too dispersed to distinguish the one kilometer scale variability of physical parameters in depth. This probably requires more sophisticated measuring devices to speed up the time of sampling. There is also a need for sampling many cores at the same site to investigate the very narrow variability.

ACKNOWLEDGMENTS

The authors sincerely acknowledge Captain Frank Cervell and his crue on the Icebreaker TOR for valuable support to and comfortable accomodation during the study. This work is a part of a Swedish-Finnish Winter Navigation Programme and has been partly financed by the Swedish National Maritime Administration and the Swedish Board for Space Activities. We also express our acknowledgements to Vera Kuylenstierna for typing and proof reading.

REFERENCES

Cox, N., and Weeks, W. (1983)
Equations for determining the gas and brine volumes in sea ice samples.
J. Glaciology, Vol. 29, No. 102

Cox, N., Richter-Menge, A., Weeks, W., Mellor, M., and Bosworth, H. (1984)
Mechanical properties of multi-year sea ice.
CRREL Reports, 84 - 9

Danielsson, G., Elfgren, L., Fransson, L., and Åström, L. (1988)
Field investigation of ice impact on light weight aggregate concrete.
Project report, Division of Structural Engineering, 614 01-2, Luleå University of Technology, Sweden

Fransson, L. (1983)
Full scale tests of the bearing capacity of a floating ice sheet.
Proc. of the Seventh International Conference on Port and Ocean Engineering under Artic Conditions.
Vol. 2, pp 687 - 697, VTT, Vuorimiehentio 5, Helsinki, Finland

Fransson, L., Håkansson, B., Omstedt, A., Stehn, L., and Åström, L. (1989)
Variation of ice properties in an ice area of 1 x 2 km in the Gulf of Bothnia.
Conference on Port and Ocean Engineering under Arctic Conditions (POAC-89), Proceeding, Vol. 3, Luleå University of Technology, Luleå, Sweden

Håkansson, B., and Thompson, T. (1988)
Ground truth data for SAR-data interpretation at study area III.
In: BEPERS PILOT STUDY, Data Report, Winter Navigation Research Board, Rep. No. 45

Leppäranta, M. (1987)
Field experiment SEA ICE-85 in mid-winter in the Bay of Bothnia.
MERI, No. 15, pp 1 - 98, Finnish Institute of Marine Research, P.O. Box 33, SF-00931 Helsinki, Finland

Maykut, G. (1986)
The surface heat and mass balance.
In: The Geophysics of Sea Ice, ed. N. Untersteiner, NATO ASI Series B: Physics, Vol. 146

Michel, B., and Hodgson, T.P. (1982)
Field measurements of ice crushing strength.
Marine Aids Division, Canada.

Michel, B. (1978)
Ice mechanics.
Les Presses de l'Université Laval, Quebec, Canada

Nakawo, M. (1983)
Measurements on air porosity of sea ice.
Annals of Glaciology, Vol. 4, pp. 204 - 208

Omstedt, A. (1985)
An investigation of the crystal structure of sea ice in the Bothnian Bay.
SMHI Reports, No. RHO 40, pp 1 - 17

Palosuo, E. (1961)
Crystal structure of brackish and fresh water ice.
International Association of Scientific Hydrology (IAHR), No. 54, General Assembly of Helsinki, 25/7 - 6/8, 1969, pp 9 - 14

Schwerdtfeger, P. (1963)
The thermal properties of sea ice.
J. Glaciology, Vol. 4, No. 36

Attachment A: Ice core classification

Attachment B: Ice core photos

Attachment C: Ice core temperature, salinity, density, and porosity

SMHI
HO
kuy/L/SCR

SMHI Rapporter, HYDROLOGI OCH OCEANOGRAFI (RHO)

Nr 1 Weil, J G
Verification of heated water jet numerical model
Stockholm 1974

Nr 2 Svensson, J
Calculation of poison concentrations from a hypothetical accident off the Swedish coast
Stockholm 1974

Nr 3 Vasseur, B
Temperaturförhållanden i svenska kustvatten
Stockholm 1975

Nr 4 Svensson, J
Beräkning av effektiv vattentransport genom Sunninge sund
Stockholm 1975

Nr 5 Bergström, S och Jönsson, S
The application of the HBV runoff model to the Filefjell research basin
Norrköping 1976

Nr 6 Wilmot, W
A numerical model of the effecta of reactor cooling water on fjord circulation
Norrköping 1976

Nr 7 Bergström, S
Development and application of a conceptual runoff model
Norrköping 1976

Nr 8 Svensson, J
Seminars at SMHI 1976-03-29--04-01 on numerical models of the spreading of cooling water
Norrköping 1976

Nr 9 Simons, J, Funkquist, L and Svensson, J
Application of a numerical model to Lake Vänern
Norrköping 1977

Nr 10 Svensson, S
A statistical study for automatic calibration of a conceptual runoff model
Norrköping 1977

Nr 11 Bork, I
Model studies of dispersion of pollutants in Lake Vänern
Norrköping 1977

Nr 12 Fremling, S
Sjöisars beroende av väder och vind, snö och vatten
Norrköping 1977

Nr 13 Fremling, S
Sjöisars bärighet vid trafik
Norrköping 1977

Nr 14 Bork, I
Preliminary model studies of sinking plumes
Norrköping 1978

Nr 15 Svensson, J and Wilmot, W
A numerical model of the circulation in Öresund
Evaluation of the effect of a tunnel between Helsingborg and Helsingör
Norrköping 1978

Nr 16 Funkquist, L
En inledande studie i Vätterns dynamik
Norrköping 1978

Nr 17 Vasseur, B
Modifying a jet model for cooling water outlets
Norrköping 1979

Nr 18 Udin, I och Mattsson, I
Havsis- och snöinformation ur datorbearbetade satellitdata - en metodstudie
Norrköping 1979

Nr 19 Ambjörn, C och Gidhagen, L
Vatten- och materialtransporter mellan Bottniska viken och Östersjön
Norrköping 1979

Nr 20 Gottschalk, L och Jutman, T
Statistical analysis of snow survey data
Norrköping 1979

Nr 21 Eriksson, B
Sveriges vattenbalans. Årsmedelvärde (1931-60) av nederbörd, avdunstning och avrinning
Norrköping 1980

Nr 22 Gottschalk, L and Krasovskaia, I
Synthesis, processing and display of comprehensive hydrologic information
Norrköping 1980

Nr 23 Svensson, J
Sinking cooling water plumes in a numerical model
Norrköping 1980

Nr 24 Vasseur, B, Funkquist, L and Paul, J F
Verification of a numerical model for thermal plumes
Norrköping 1980

Nr 25 Eggertsson, L-E
HYPOS - ett system för hydrologisk positionsangivelse
Norrköping 1980

Nr 26 Buch, Erik
Turbulent mixing and particle distribution investigations in the Himmerfjärd 1978
Norrköping 1980

Nr 27 Eriksson, B
Den "potentiella" evapotranspirationen i Sverige
Norrköping 1980

Nr 28 Broman, B
On the spatial representativity of our oceanographic measurements
Norrköping 1981

Nr 29 Ambjörn, C, Luide, T, Omstedt, A, Svensson, J
En operationell oljedriftsmodell för norra Östersjön
Norrköping 1981

Nr 30 Svensson, J
Vågdata från svenska kustvatten 1979 - 1980
Norrköping 1981

Nr 31 Jutman, T
Stationsnät för vattenföring
Norrköping 1981

Nr 32 Omstedt, A, Sahlberg, J
Vertical mixing and restratification in the Bay of Bothnia during cooling
Norrköping 1982

Nr 33 Brandt, M
Sedimenttransport i svenska vattendrag
Norrköping 1982

Nr 34 Bringfelt, B
A forest evapotranspiration model using synoptic data
Norrköping 1982

Nr 35 Bhatia, P K, Bergström, S, Persson, M
Application of the distributed HBV-6 model to the Upper Narmada Basin in India
Norrköping 1984

Nr 36 Omstedt, A
A forecasting model for water cooling in the Gulf of Bothnia and Lake Vänern
Norrköping 1984

Nr 37 Gidhagen, L
Coastal upwelling in the Baltic - a presentation of satellite and in situ measurements of sea surface temperatures indicating coastal upwelling
Norrköping 1984

Nr 38 Engqvist, A, Svensson, J
Water turnover in Himmerfjärd 1977 - a simulation study
Norrköping 1984

Nr 39 Funkquist, L, Gidhagen, L
A model for pollution studies in the Baltic Sea
Norrköping 1984

Nr 40 Omstedt, A
An Investigation of the crystal structure of sea ice in the Bothnian Bay
Norrköping 1985

SMHI Rapporter, OCEANOGRAFI (RO)

Nr 1 Gidhagen, Lars, Funkquist, Lennart, and Murthy, Ray
Calculations of horizontal exchange coefficients using Eulerian time series current meter data from the Baltic Sea.
Norrköping 1986

Nr 2 Thompson, Thomas
Ymer-80, satellites, arctic sea ice and weather.
Norrköping 1986

Nr 3 Carlberg, Stig, et al.
Program för miljökvalitetsövervakning - PMK.
Norrköping, 1986

Nr 4 Lundqvist, Jan-Erik, och Omstedt, Anders
Isförhållandena i Sveriges södra och västra farvatten.
Norrköping, 1986

Nr 5 Carlberg, Stig R., Engström, Sven, Fonselius, Stig H., Palmén, Håkan, Thelén, Eva-Gun, Fyrberg, Lotta, och Yhlen, Bengt
Program för miljökvalitetsövervakning - PMK.
Utsjöprogram under 1986.
Göteborg, 1987

Nr 6 Valderrama, Jorge C.
Results of a five year survey of the distribution of urea in the Baltic Sea.
Göteborg, 1987

Nr 7 Carlberg, Stig, Engström, Sven, Fonselius, Stig, Palmén, Håkan, Thelén, Eva-Gun, Fyrberg, Lotta, och Yhlén, Bengt.
Program för miljökvalitetsövervakning - PMK.
Utsjöprogram under 1987.
Göteborg 1988

Nr 8 Håkansson, Bertil
Ice reconnaissance and forecasts in Storfjorden, Svalbard.
Norrköping 1988

Nr 9 Carlberg, Stig, Engström, Sven, Fonselius, Stig, Fyrberg, Lotta, Juhlin, Bo, Palmén, Håkan, Szaron, Jan, Thelén, Eva-Gun, Yhlén, Bengt och Zagradkin, Danuta
National Swedish programme for monitoring of environmental quality - Open sea programme. Report from activities in 1988.
Norrköping 1989

Nr 10 Fransson, L., Håkansson, B., Omstedt, A., Stehn, L.
Sea ice properties studied from the icebreaker Tor during BEPERS-88.
Norrköping 1989

<u>Pris för nedanstående publikationer</u>

Vattenföringsbestämmelser vid vattenundersökningar	100:-
Vattenföringen i Sverige	250:-
Sjöregistret	250:-
Vattendragsregistret	150:-

Attachment A

ICE CORE CLASSIFICATION

Date : 880302
Station : T1A

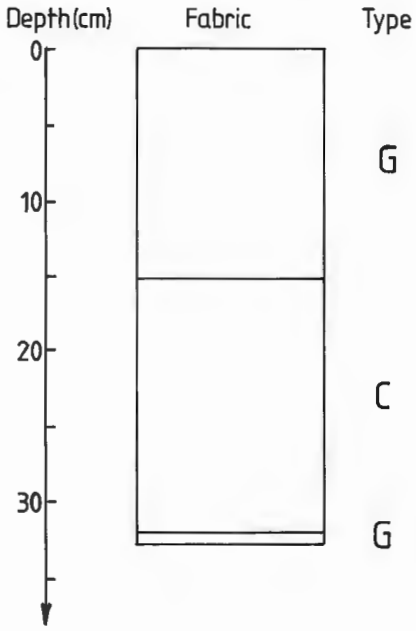

Date : 880302
Station : T1B

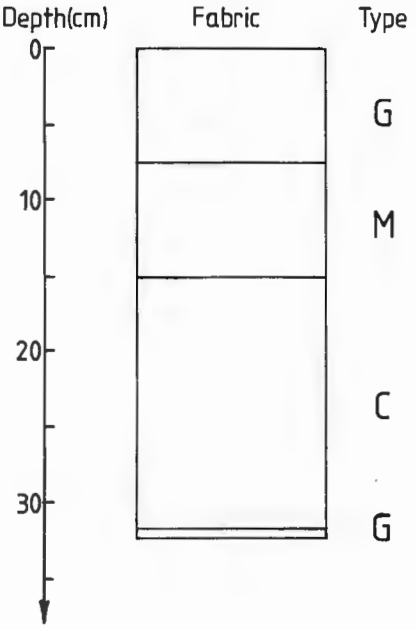

Date : 880302
Station : T1C

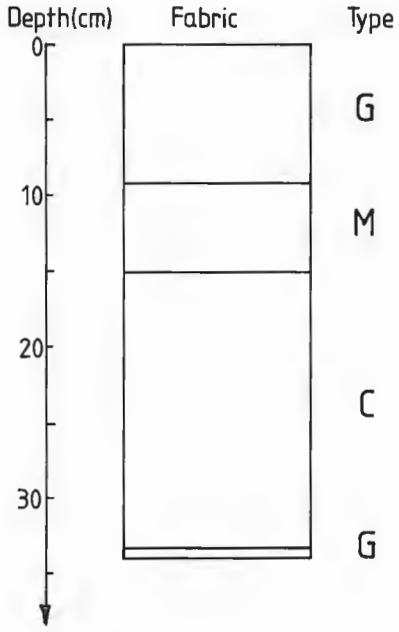

Date : 880302
Station : T2

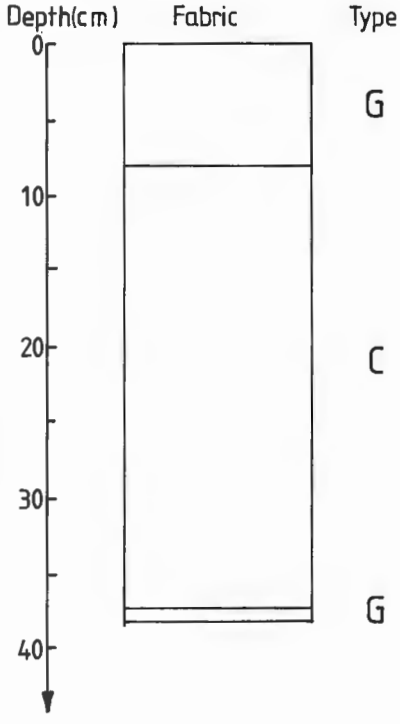

Date : 880303
Station : T3

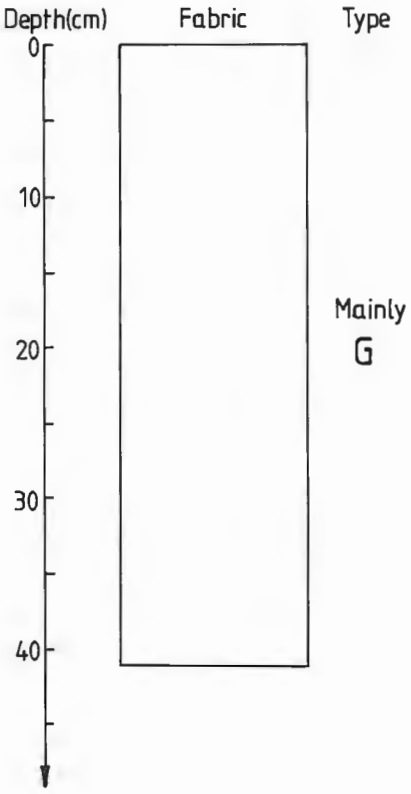

Date : 880304
Station : AB1

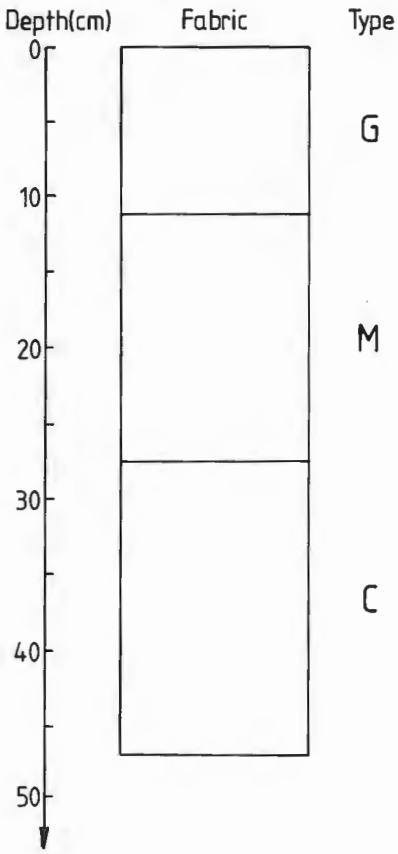

Date : 880304
Station : AB3

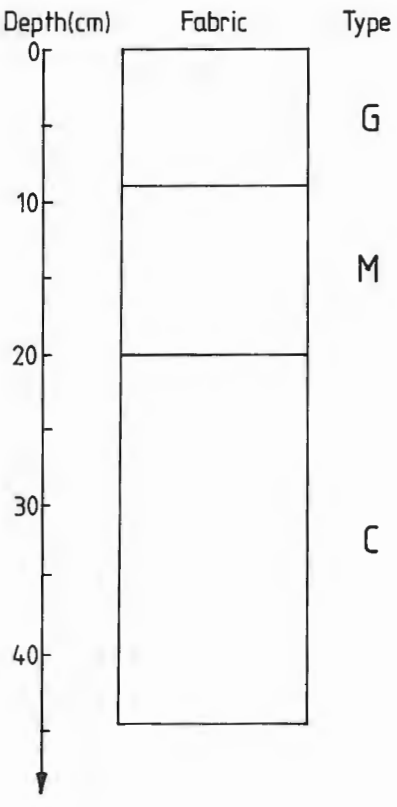

Date : 880305
Station : AB5

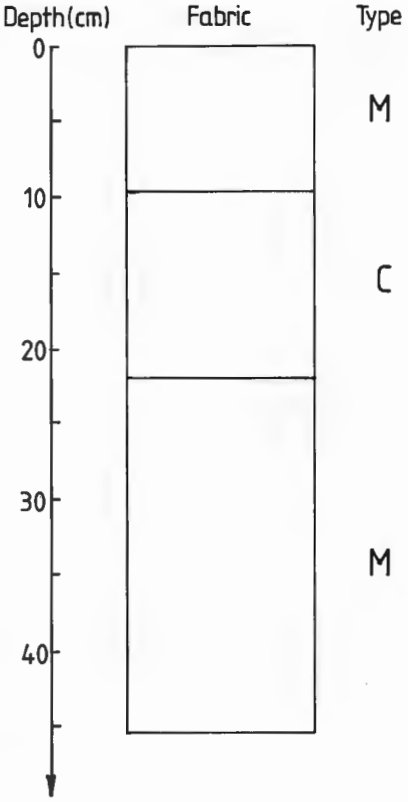

Date : 880305
Station : AB7

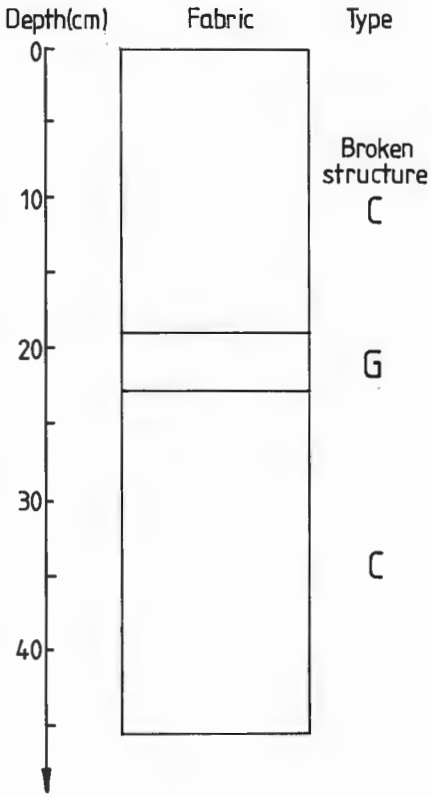

Date : 880309
Station : AB9

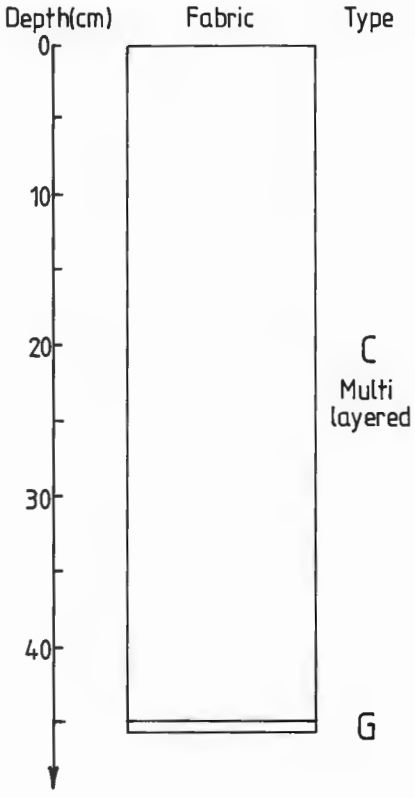

Date : 880309
Station : CD1

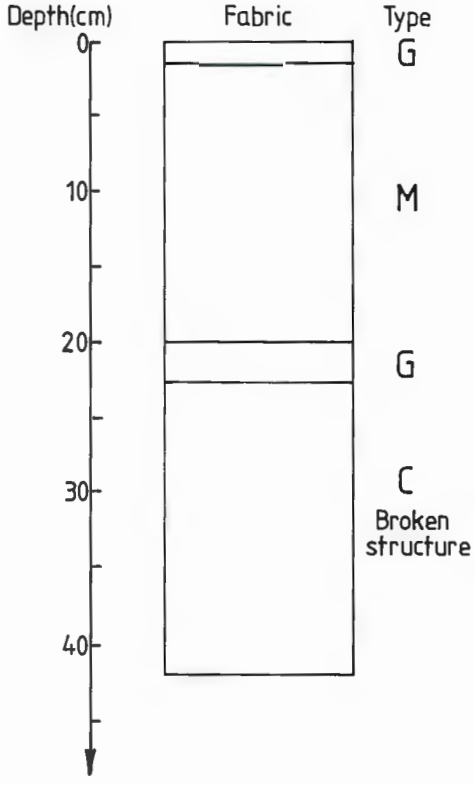

Date : 880309
Station : BC3

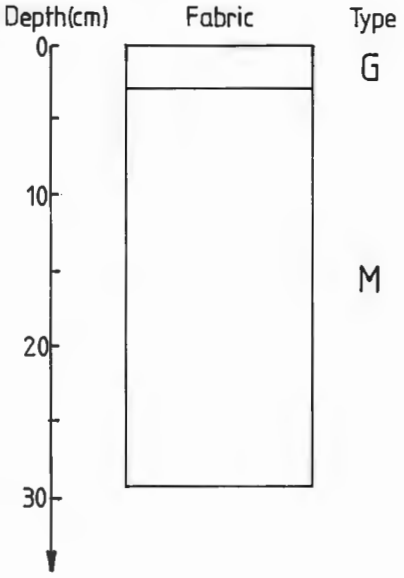

Date : 880309
Station : CD3

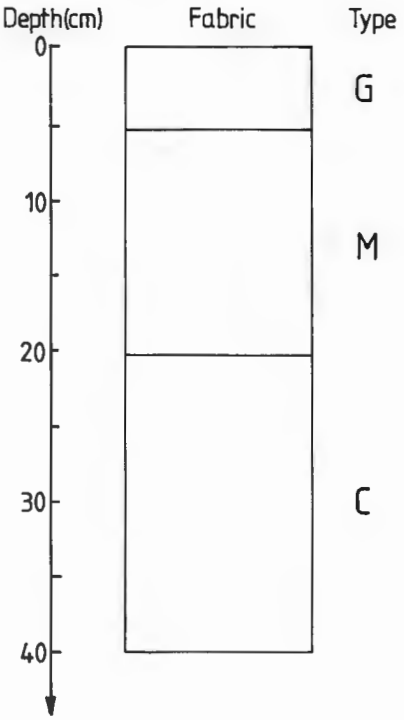

Date : 880305
Station : CD5

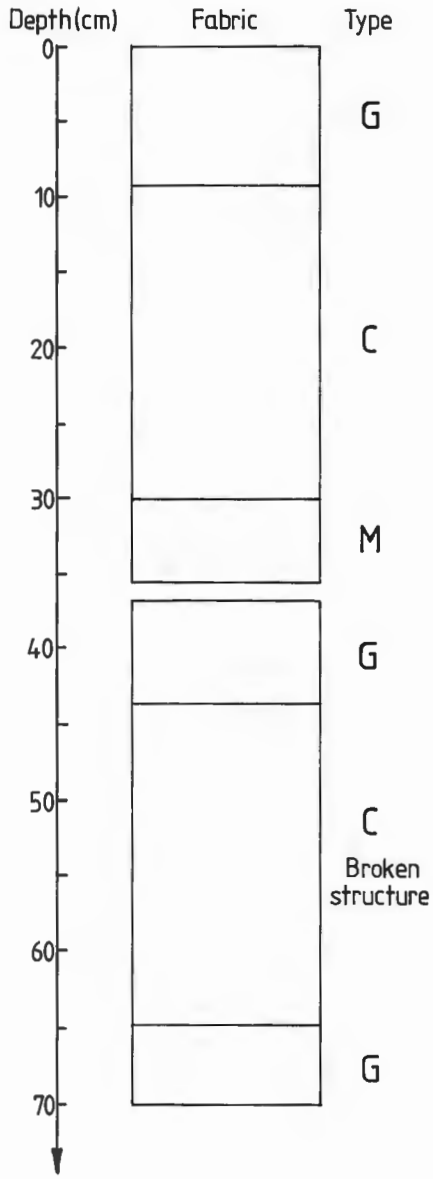

Date : 880305
Station : CD7

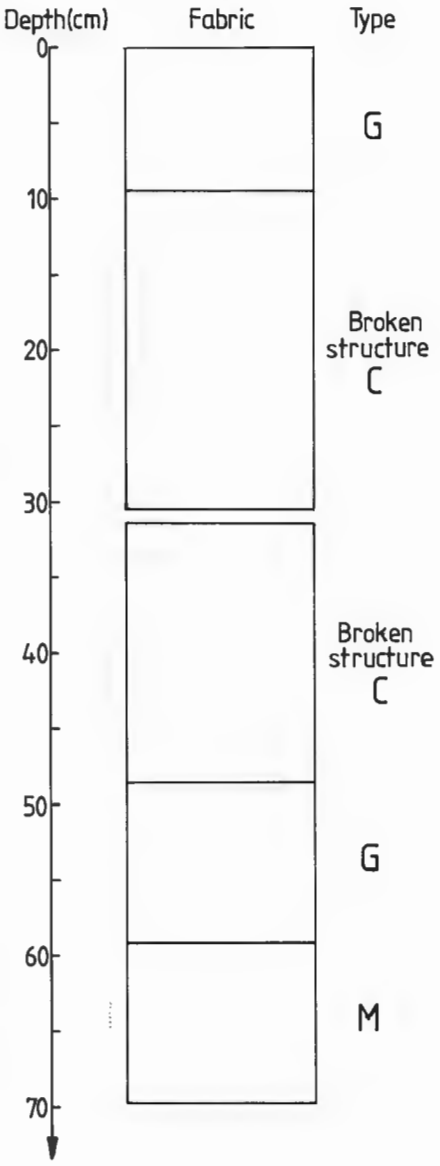

Date : 880305
Station : DA3

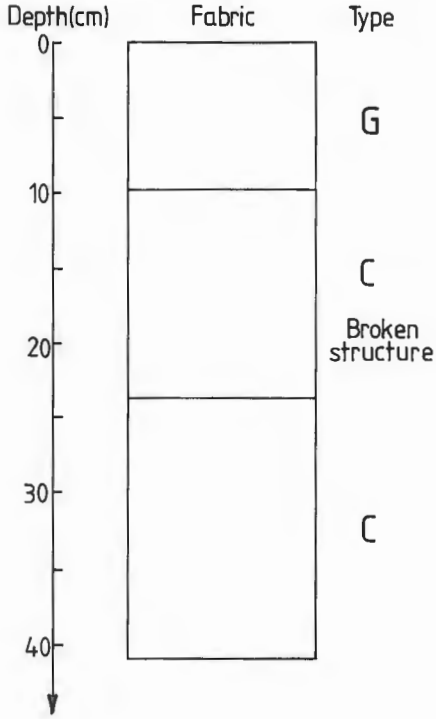

Date : 880305
Station : CD9

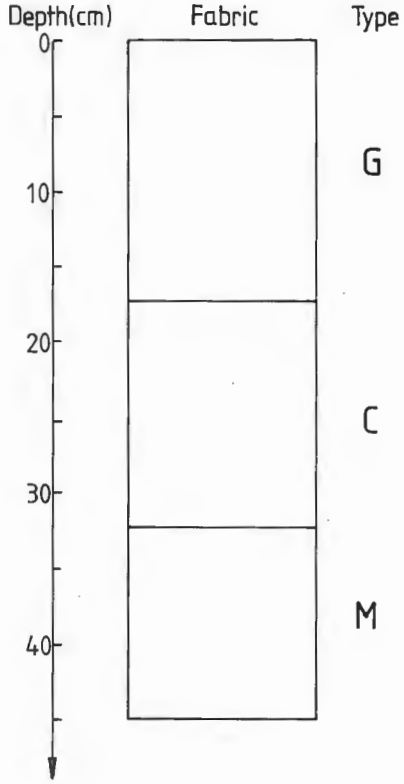

Date : 880309
Station : X

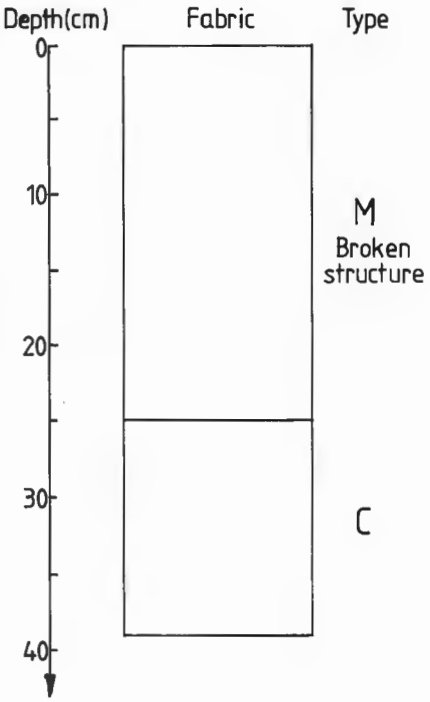

Date : 880306
Station : S30

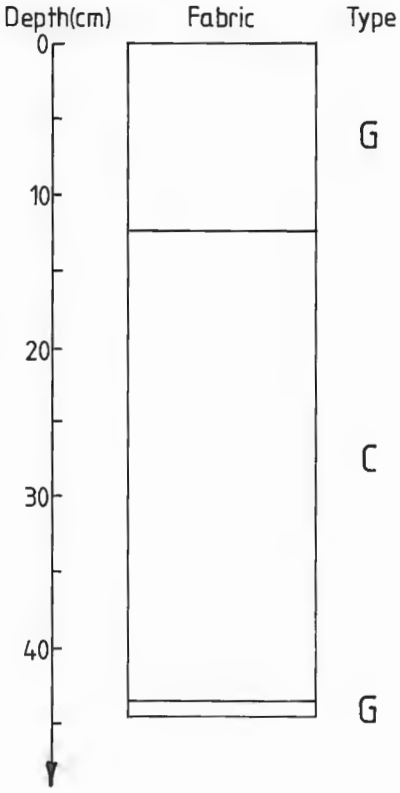

Date : 880306
Station : S70

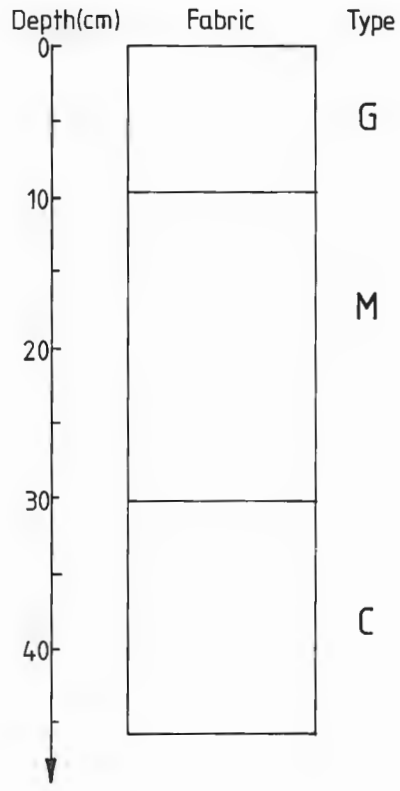

Date : 880306
Station : S50

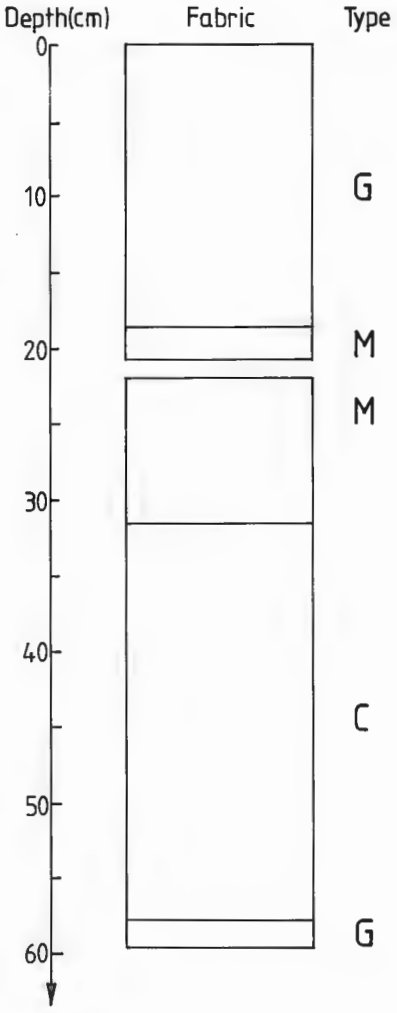

Date : 880308
Station : T25

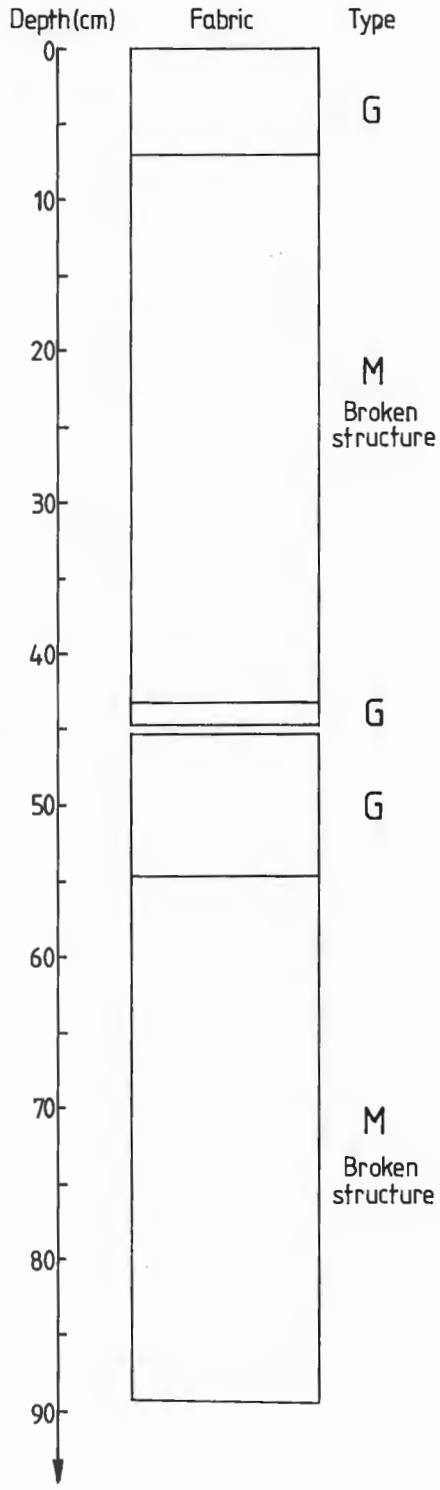

Date : 880308
Station : T55

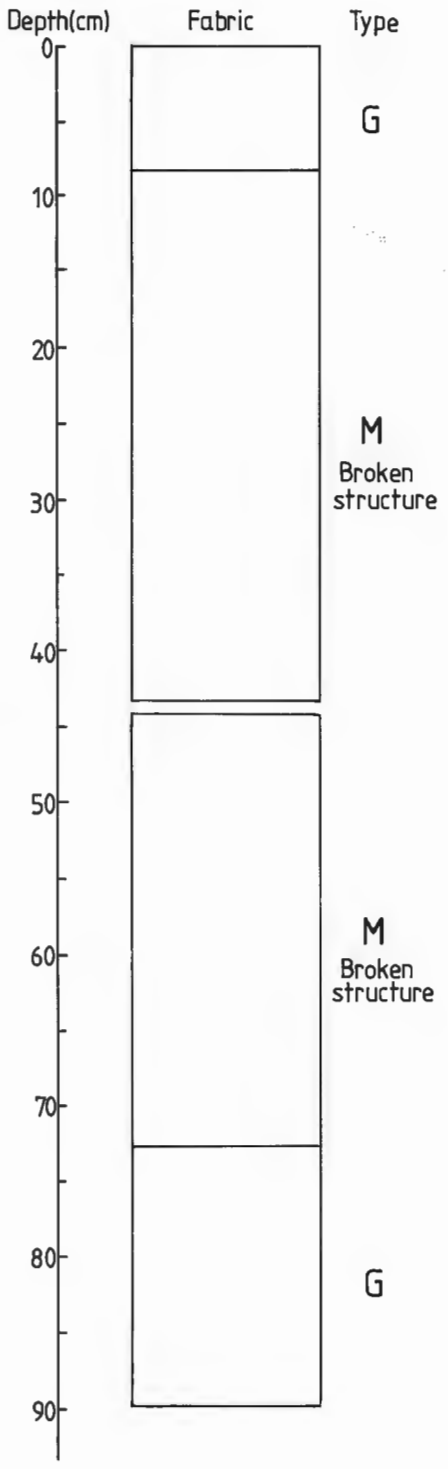

Date : 880309
Station : T75

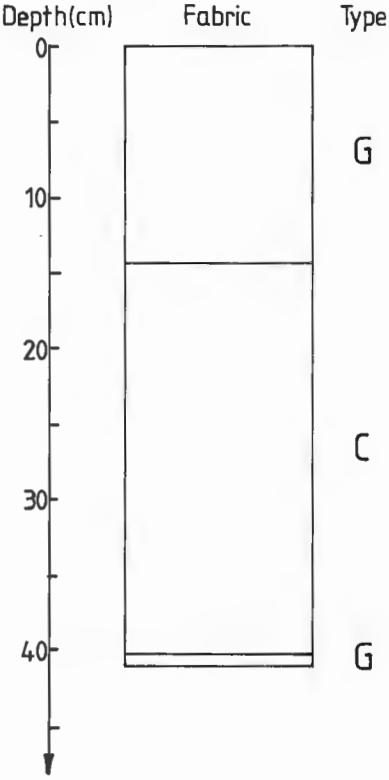

Date : 880310
Station : 10

Depth(cm) Type

0
10 M
20 C

Date : 880310
Station : 11

Depth(cm) Type

0
10 M
20

Date : 880310
Station : 12

Depth(cm) Type

0 G
10

Date : 880310
Station : 20

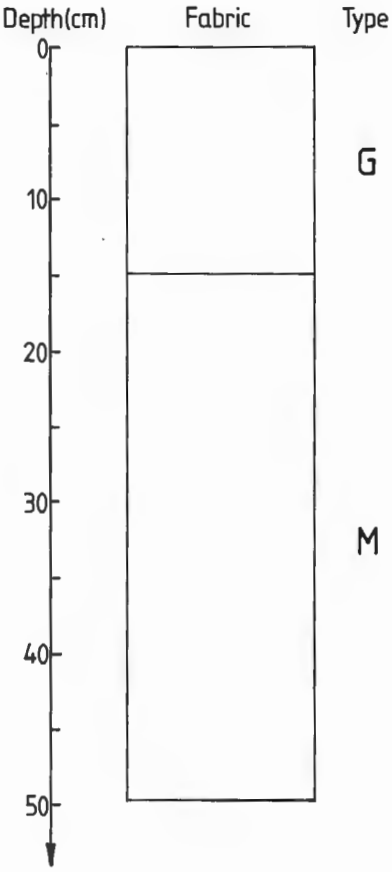

Date : 880310
Station : 23

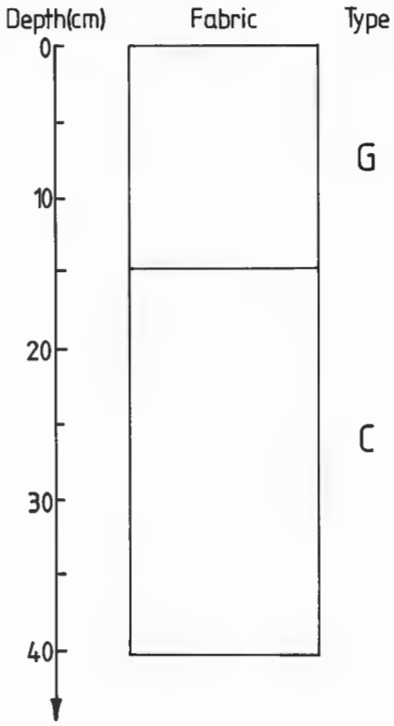

Attachment B

ICE CORE PHOTOGRAPHICS WITH LOCATIONS

Date : 880302
Station: T 1A

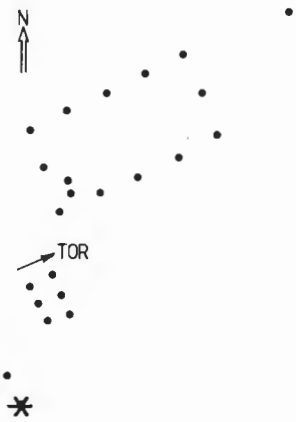

Date : 880302
Station : T1B

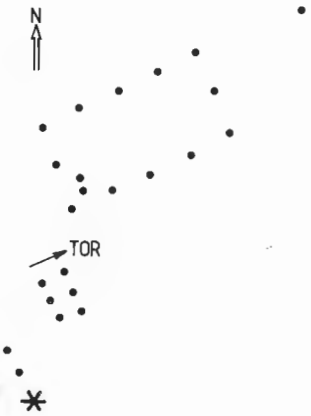

Date : 880302
Station : T1 C

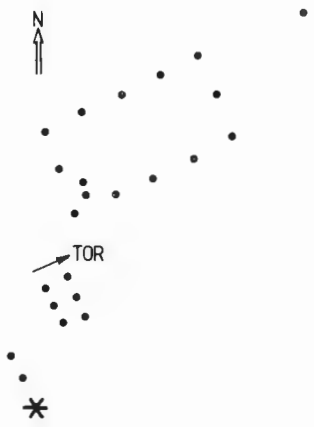

Date : 880302
Station : T 2

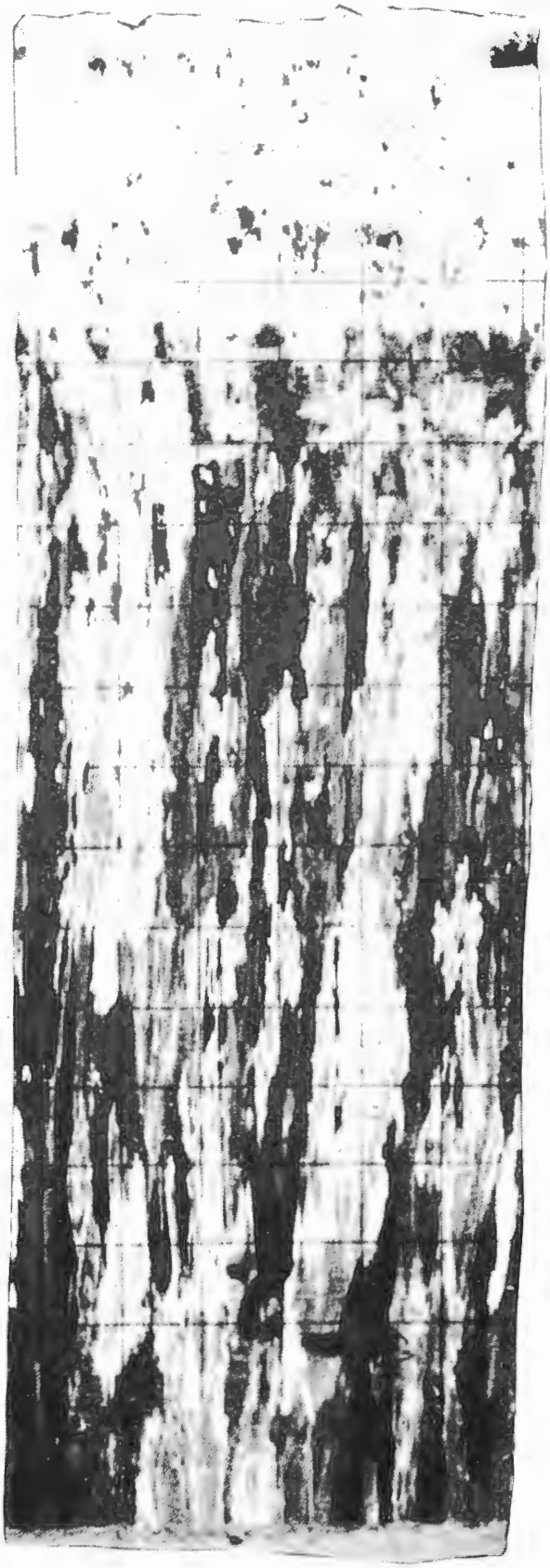

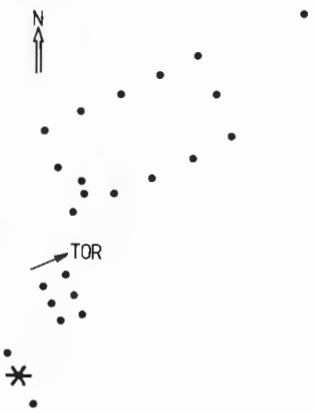

Date : 880303
Station: T 3

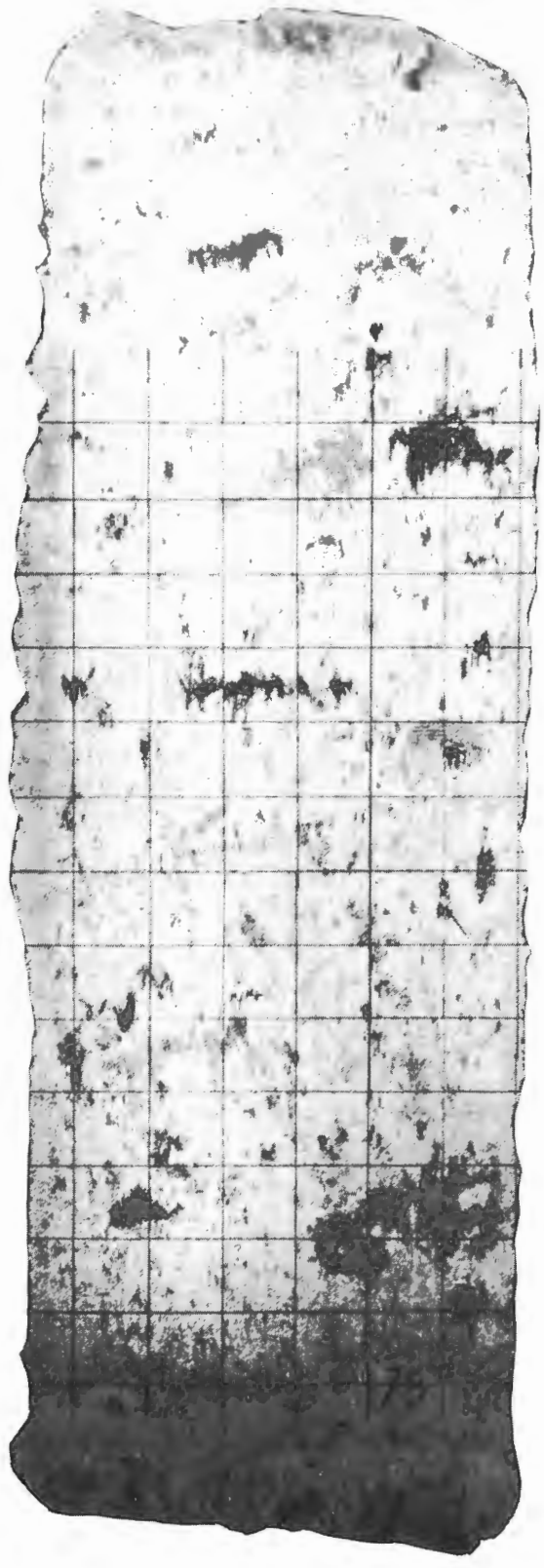

Date : 880304
Station: AB 1

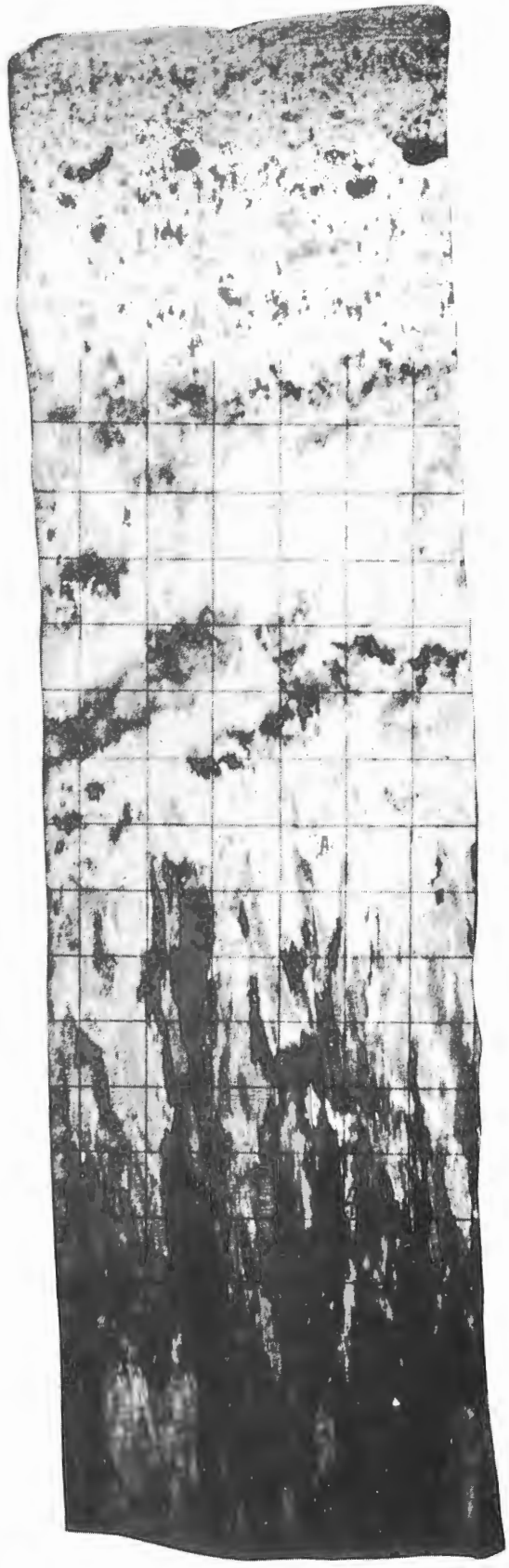

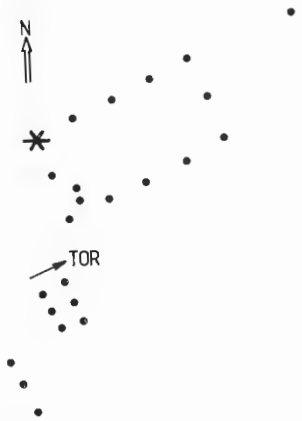

Date : 880304
Station : AB 3

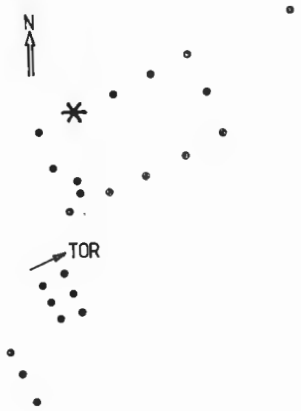

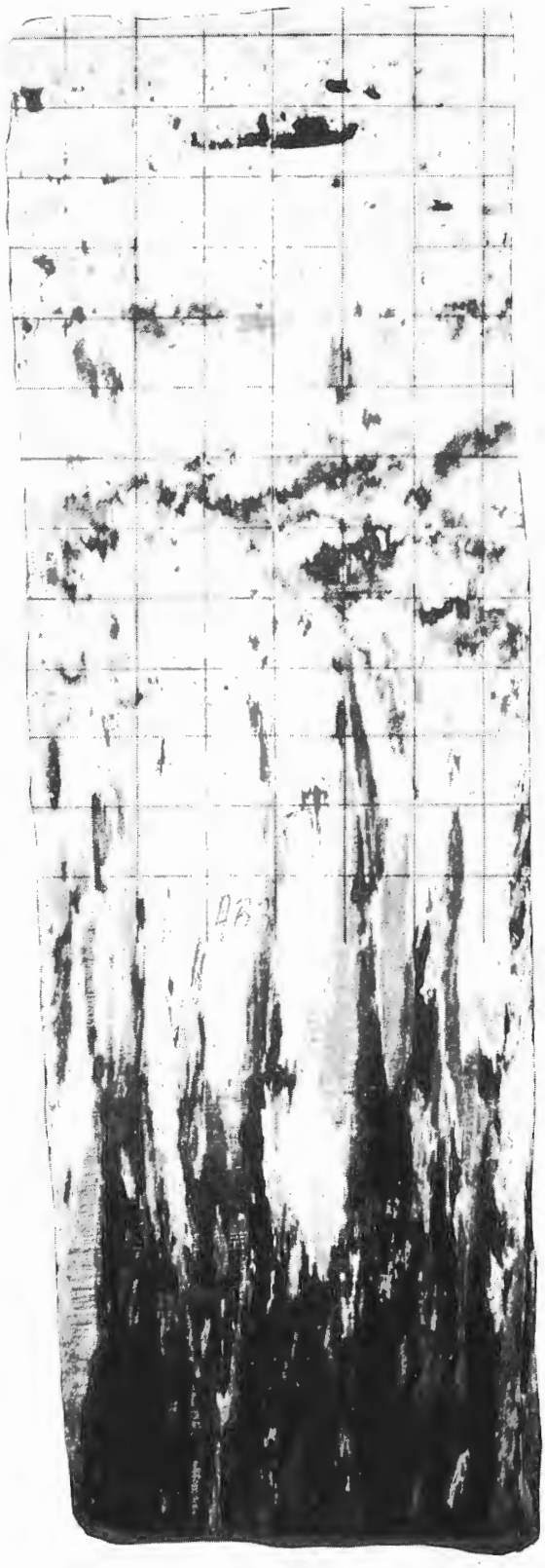

Date : 880305

Station: AB 5

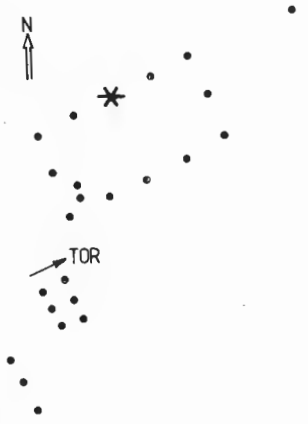

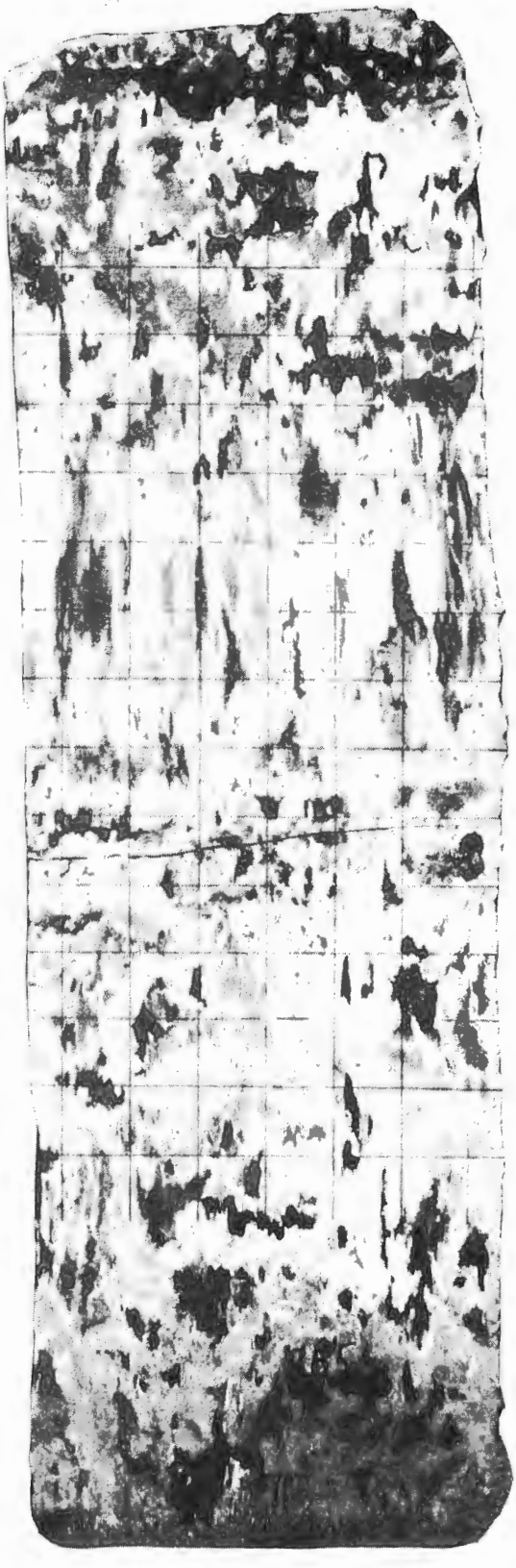

Date : 880305

Station: AB 7

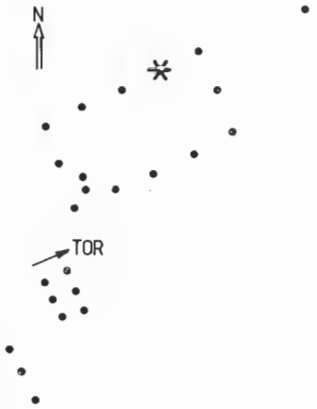

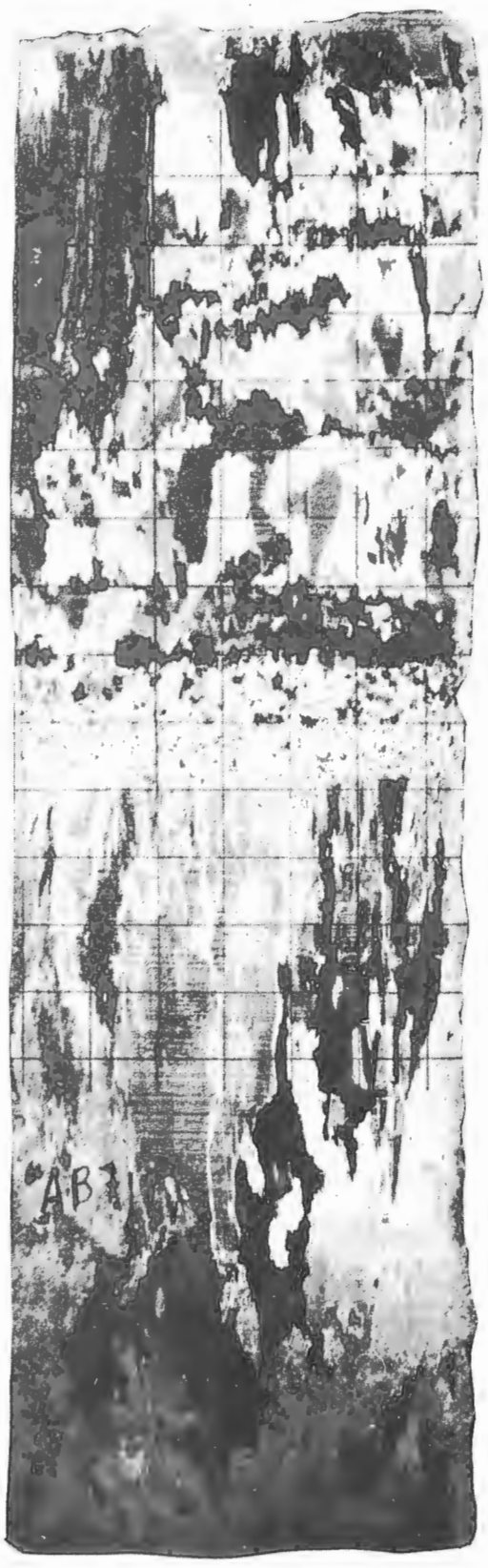

Date : 880309

Station: AB 9

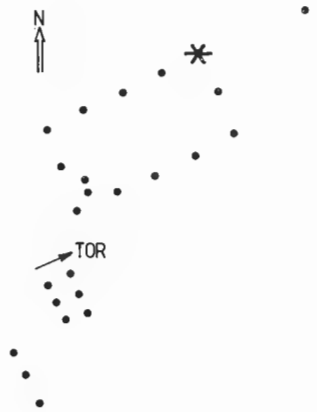

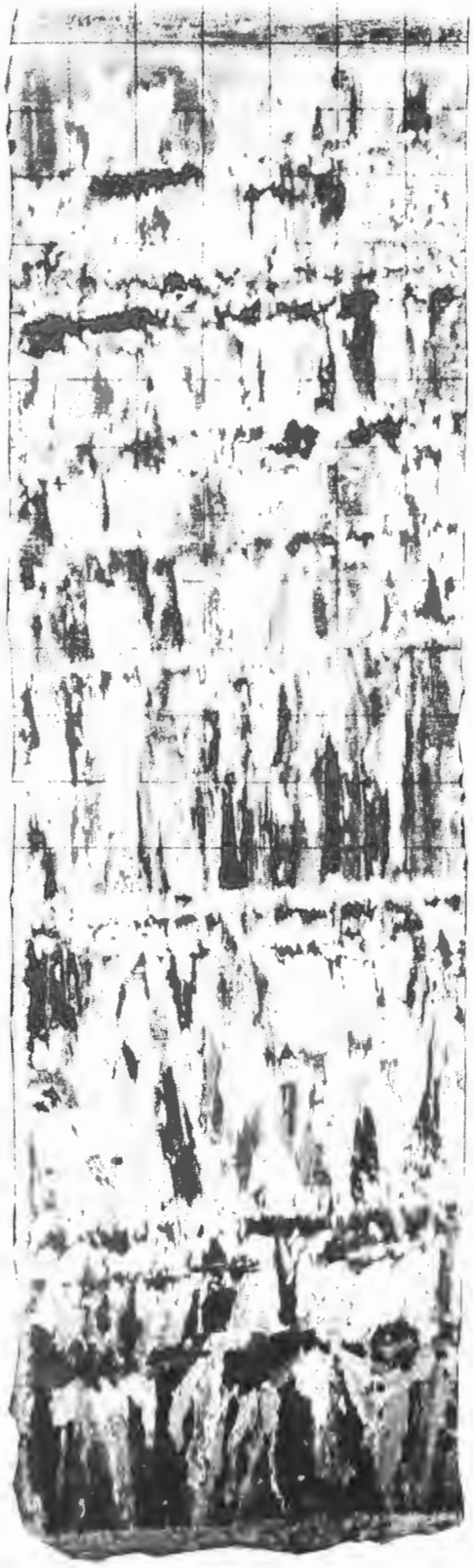

Date : 880309

Station: CD 1

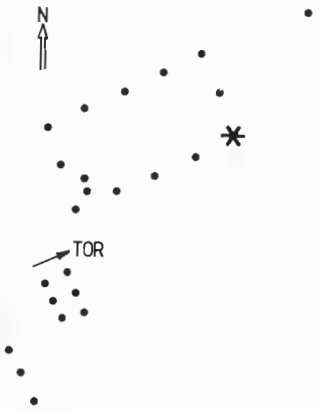

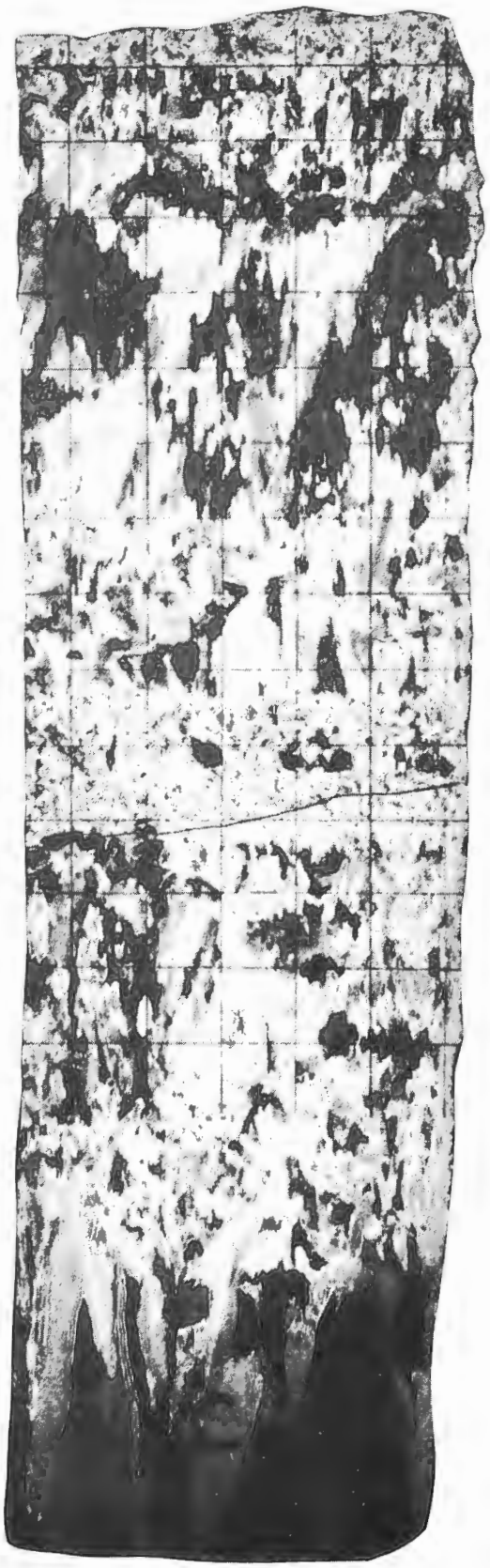

Date : 880309

Station: BC 3

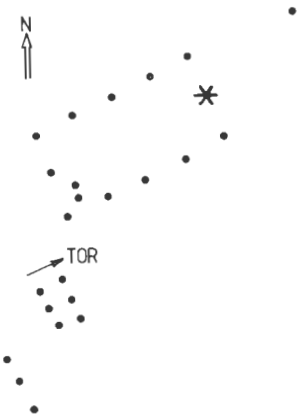

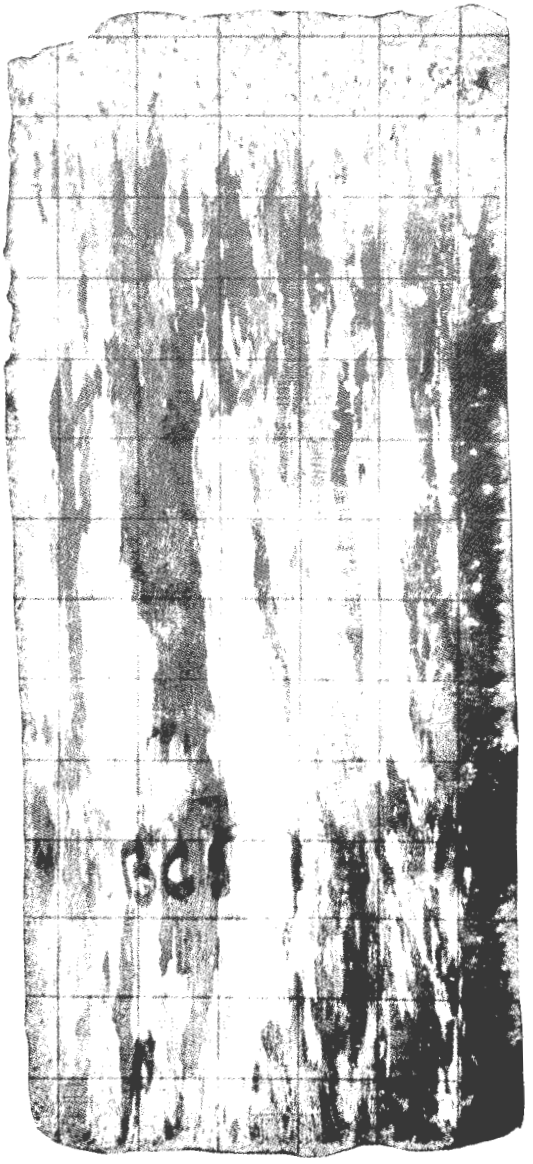

Date : 880309

Station: CD 3

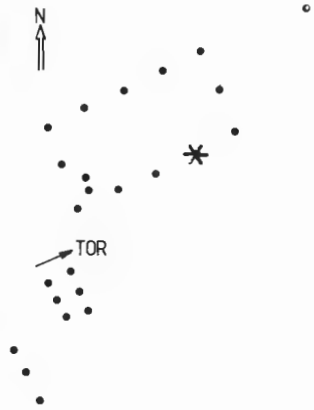

Date : 880305

Station: CD 5 Top

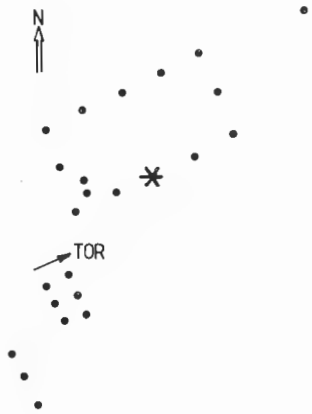

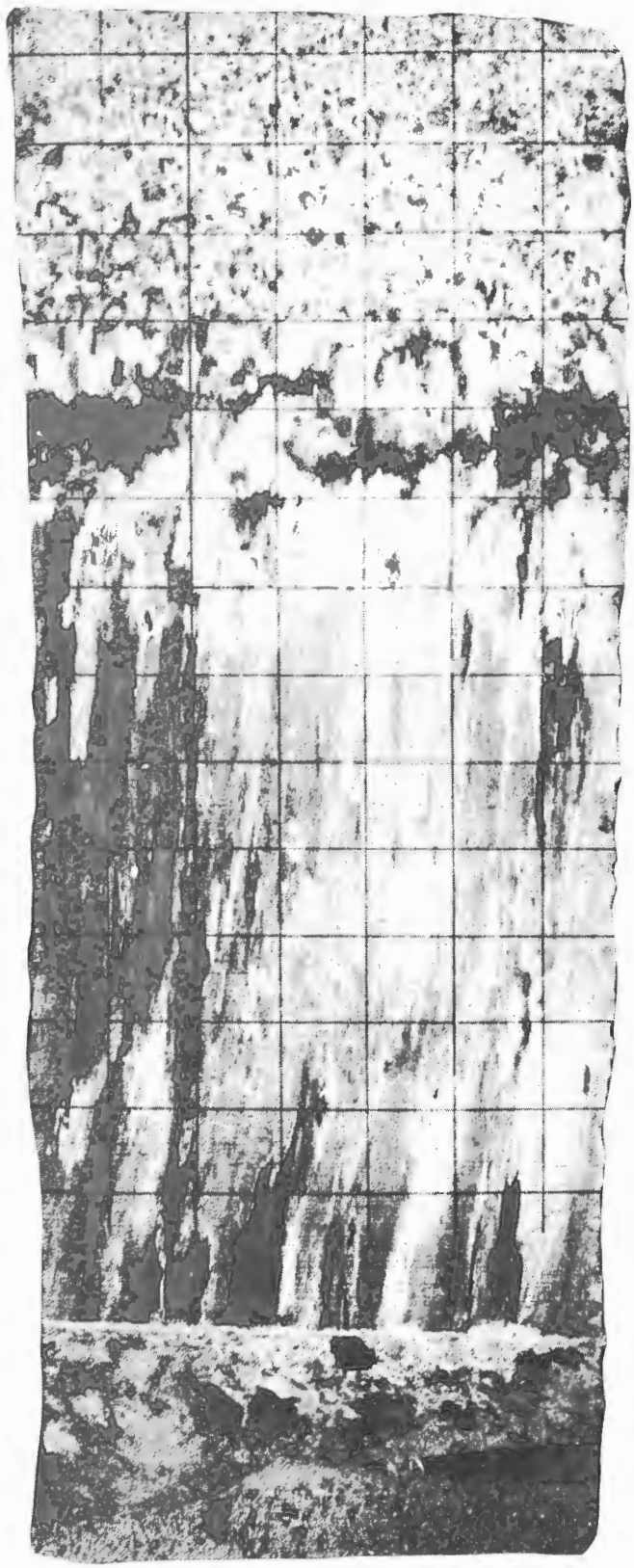

Date : 880305

Station: CD 5 Bot

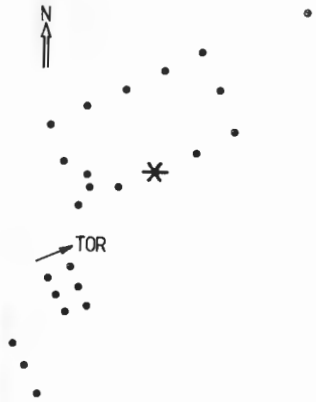

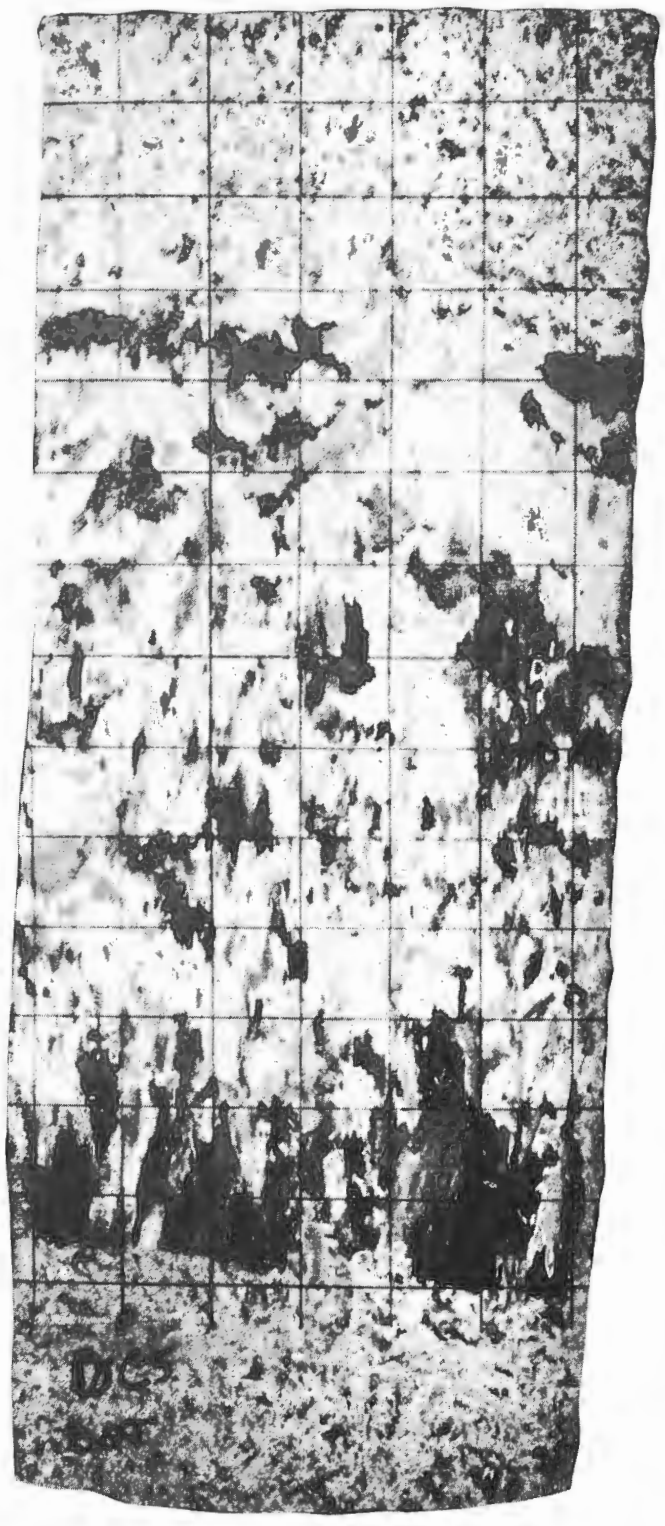

Date : 880305

Station: CD7 Top

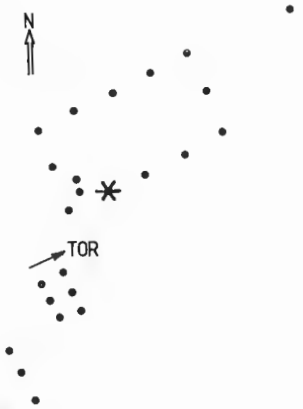

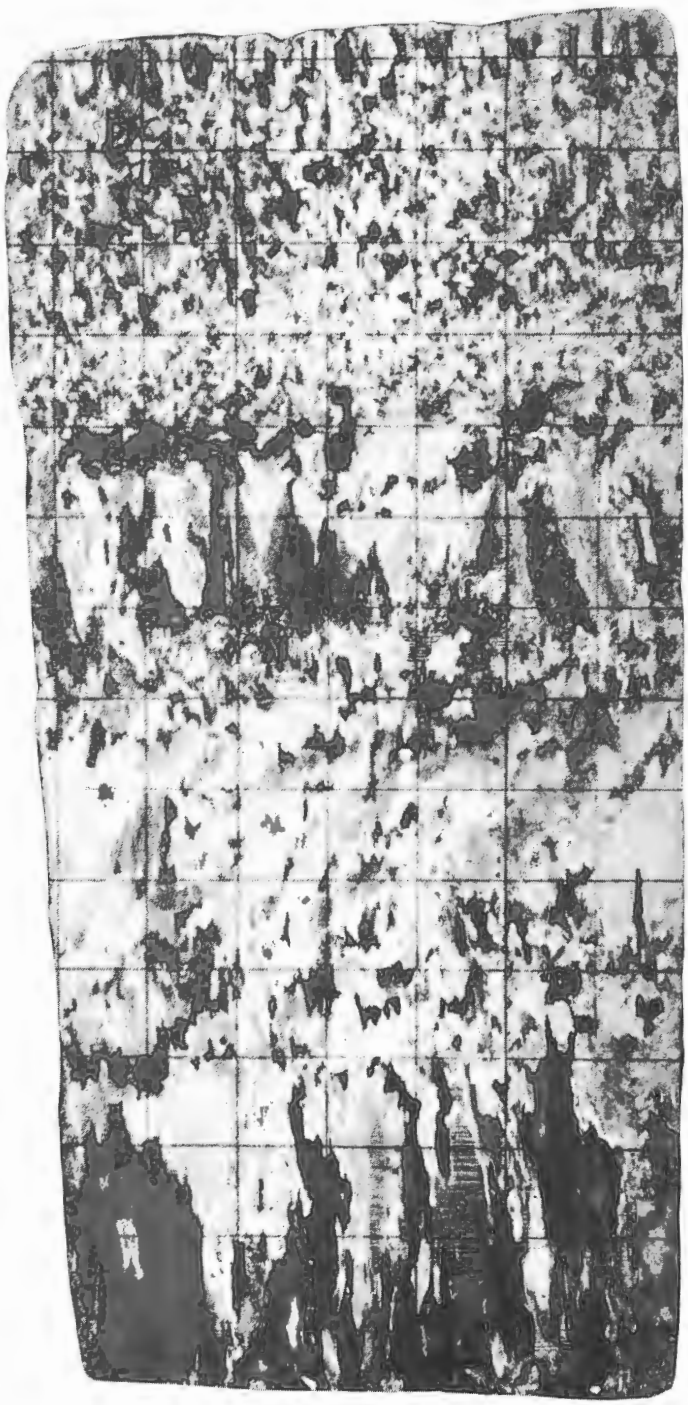

Date : 880305

Station : CD7 Bot

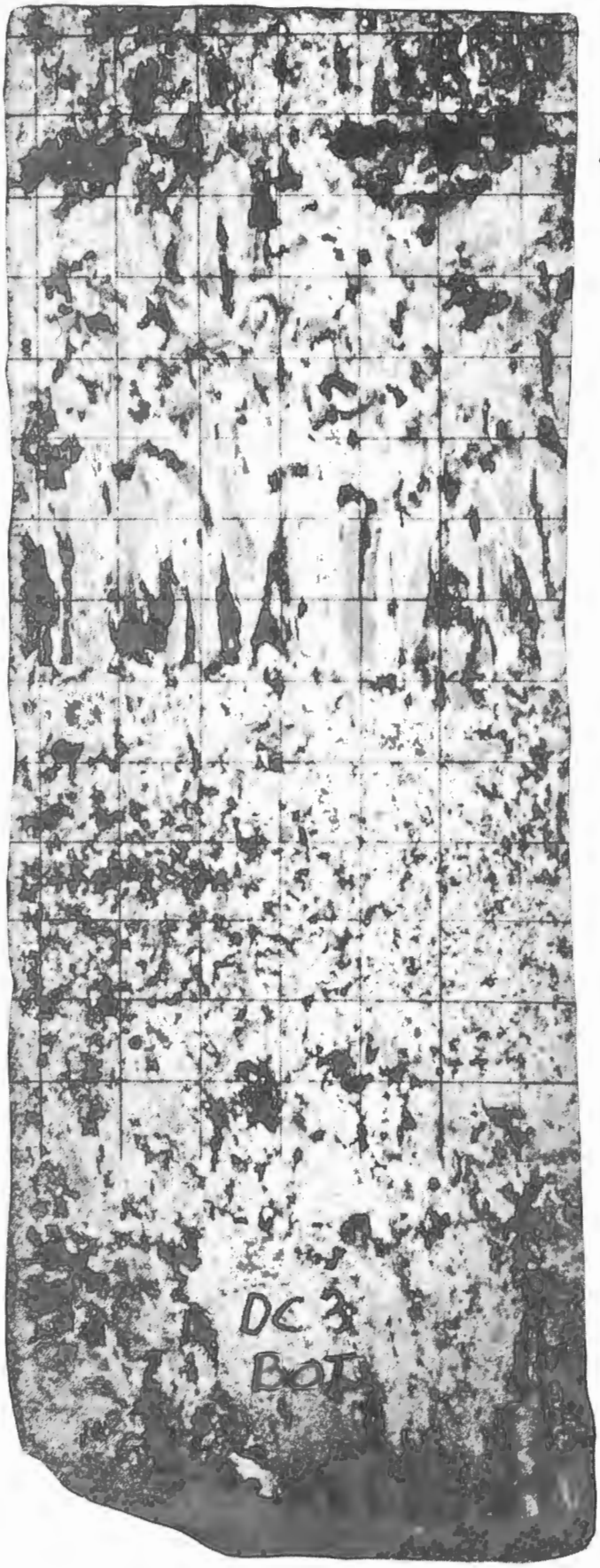

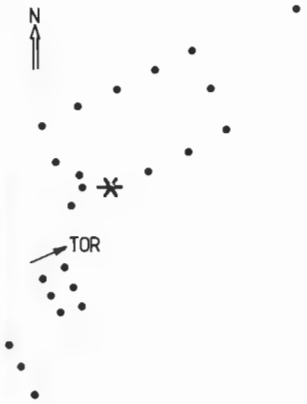

Date : 880305

Station: CD 9

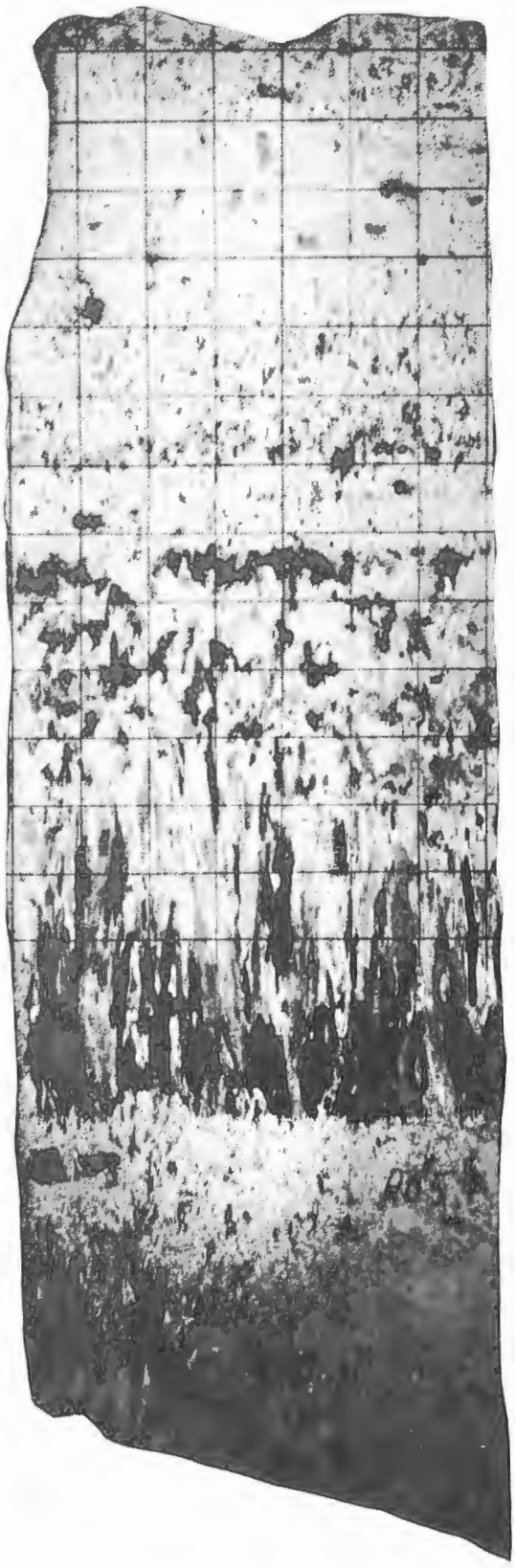

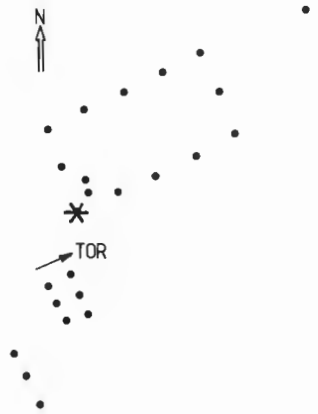

Date : 880305

Station: DA 3

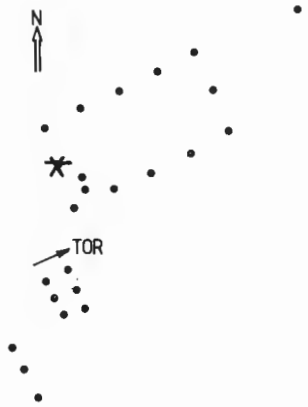

Date : 880309

Station: X

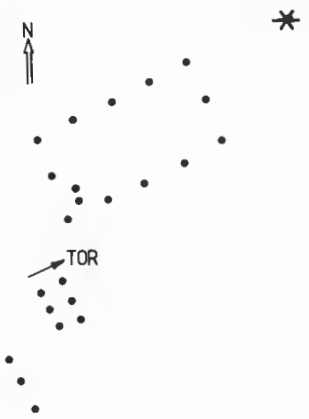

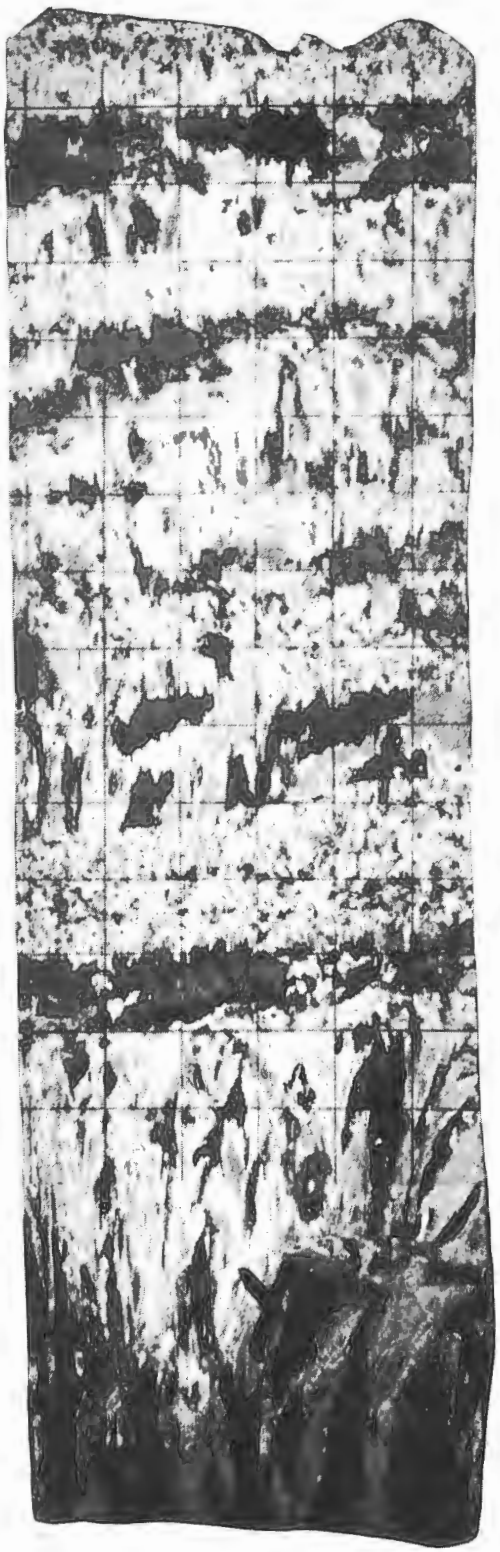

Date : 880306

Station: S 30

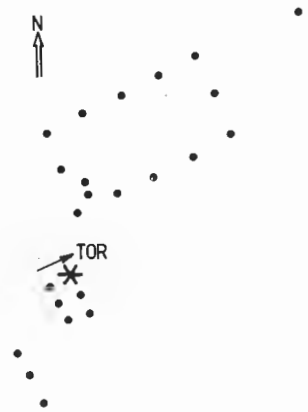

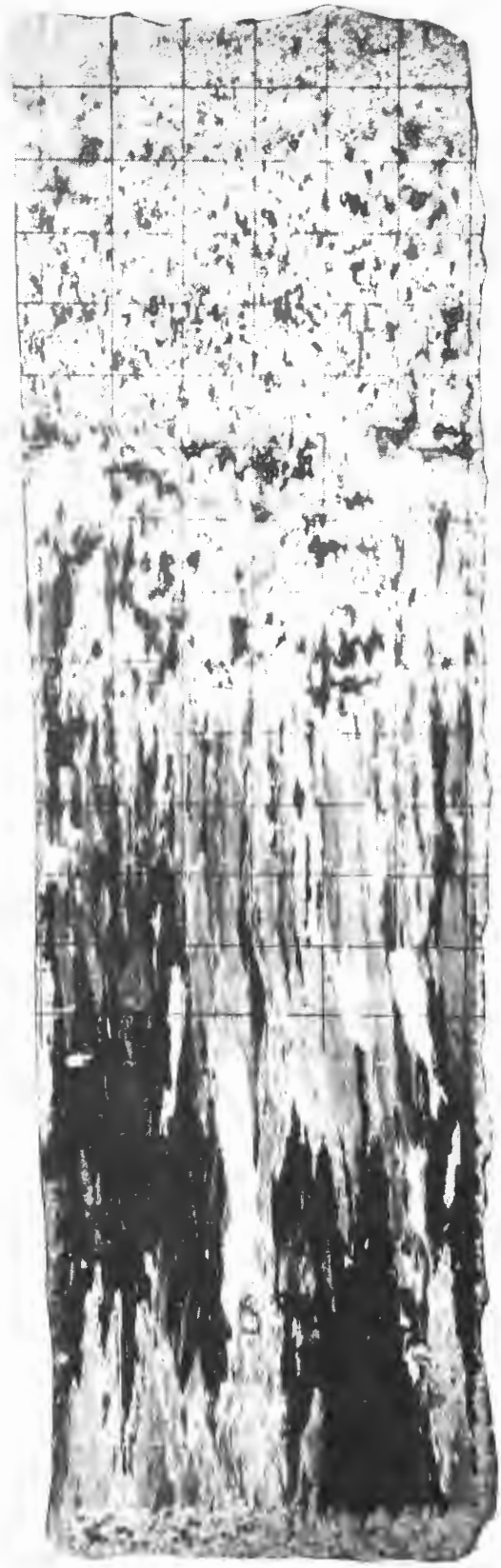

Date : 880306

Station: S 50 Top

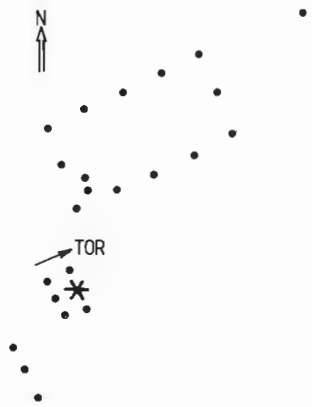

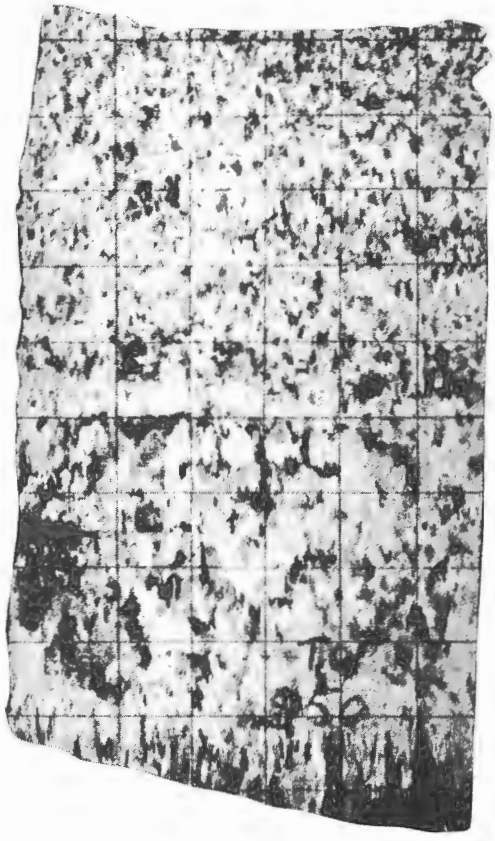

Date : 880306

Station : S 50 Bot

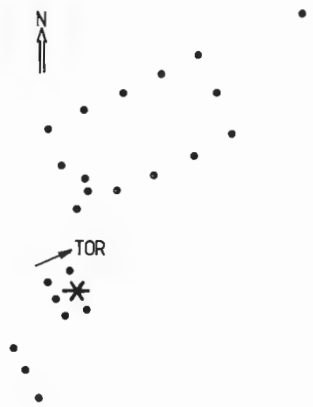

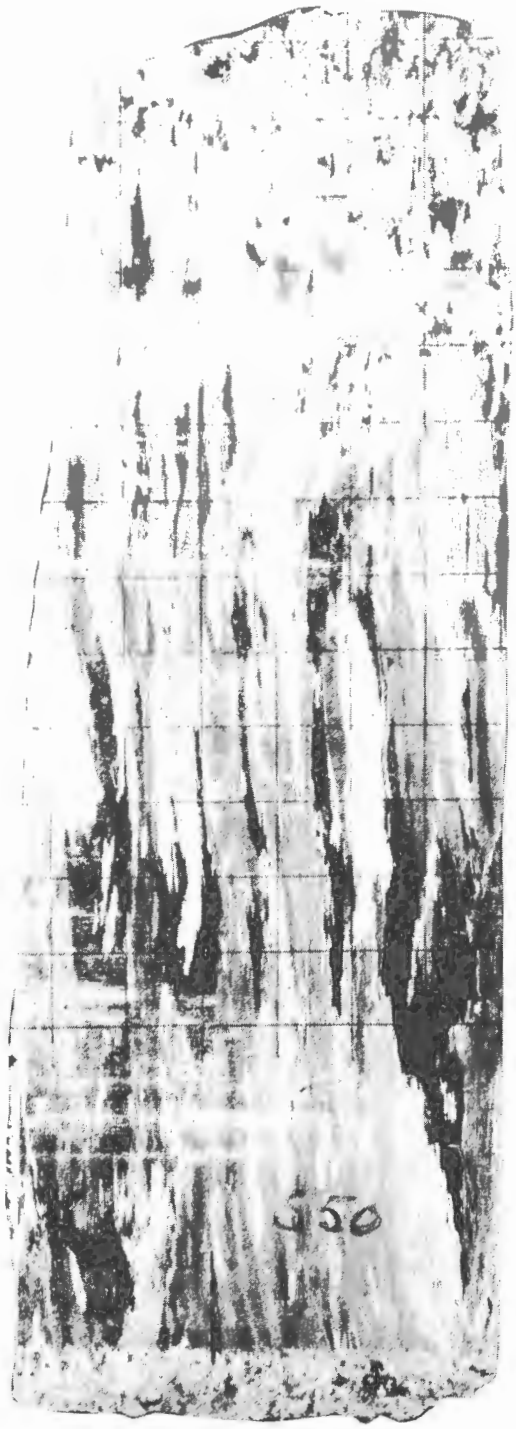

Date : 880306

Station: S 70

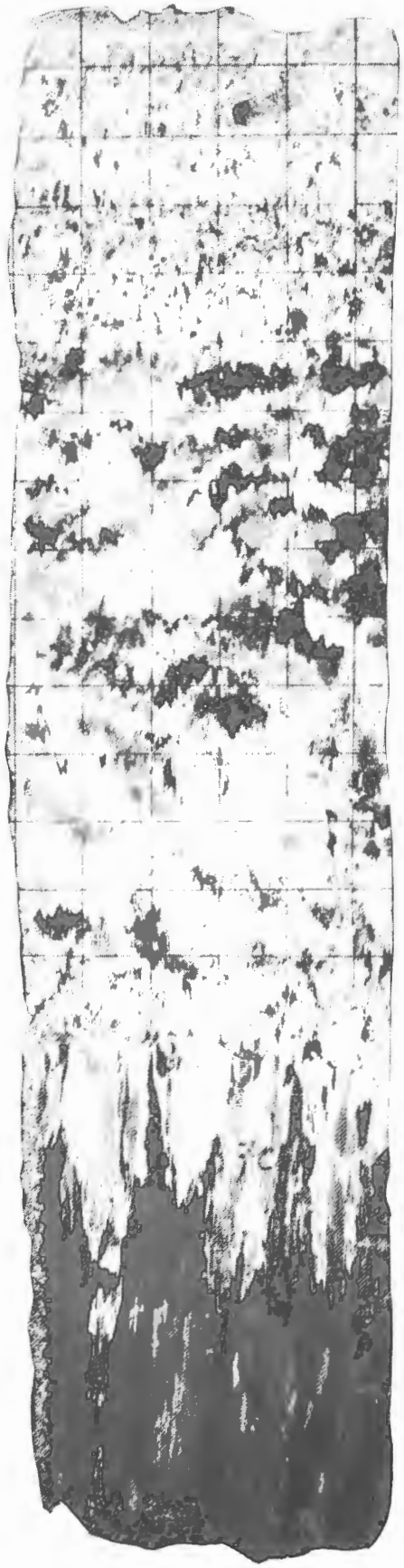

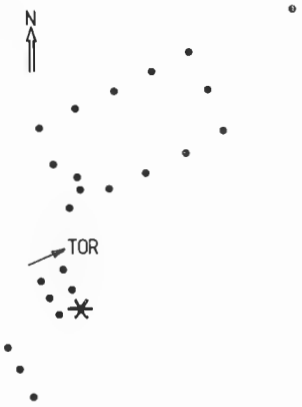

Date : 880308

Station: T 25 Top

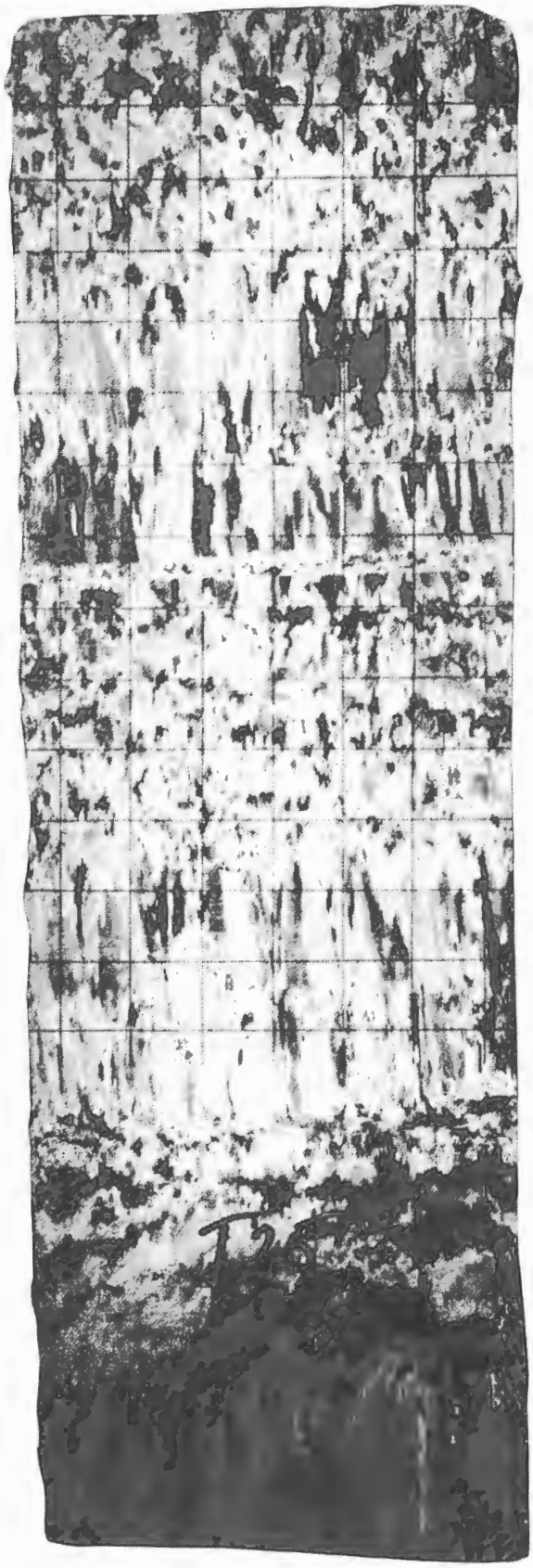

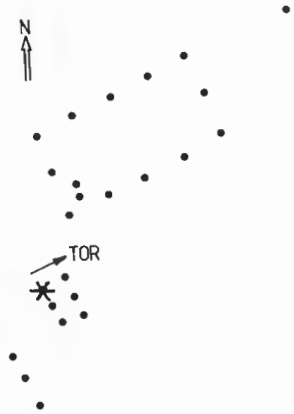

Date : 880308

Station : T 25 Bot

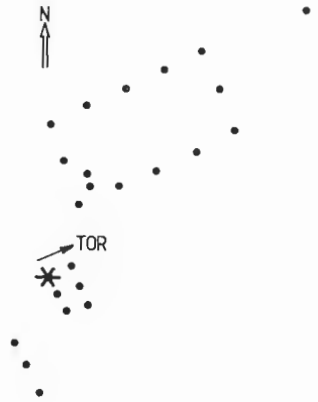

Date : 880308

Station: T 55 Top

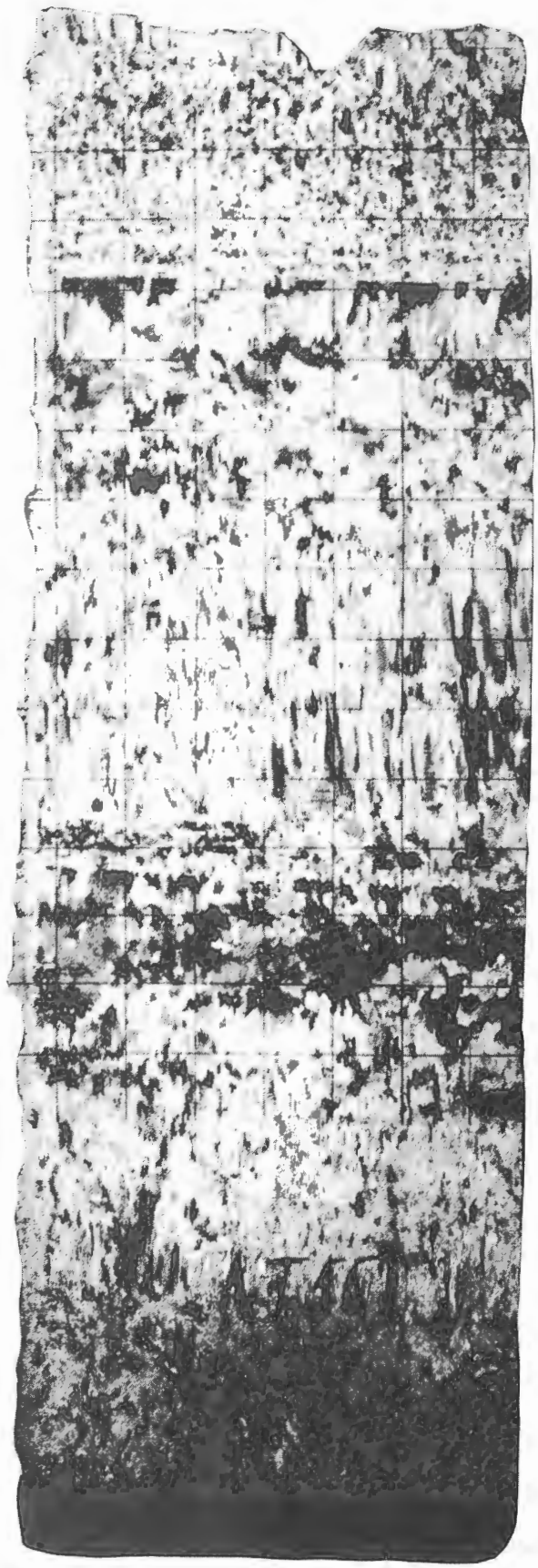

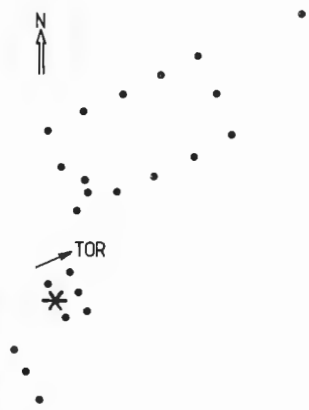

Date : 880308

Station: T55 Bot

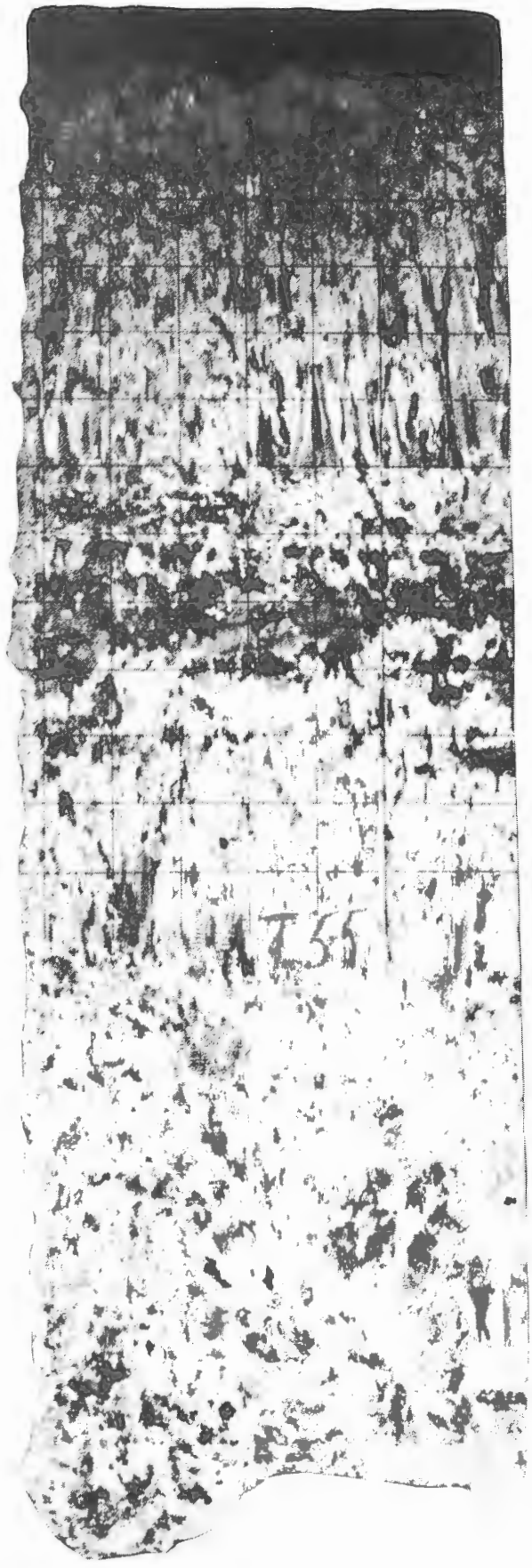

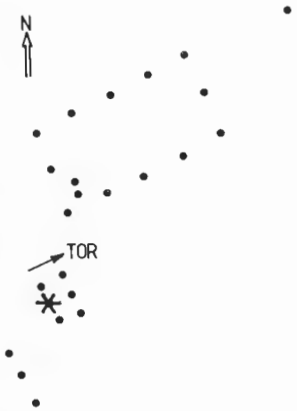

Date : 880309

Station: T 75

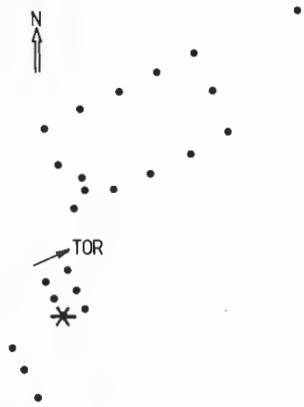

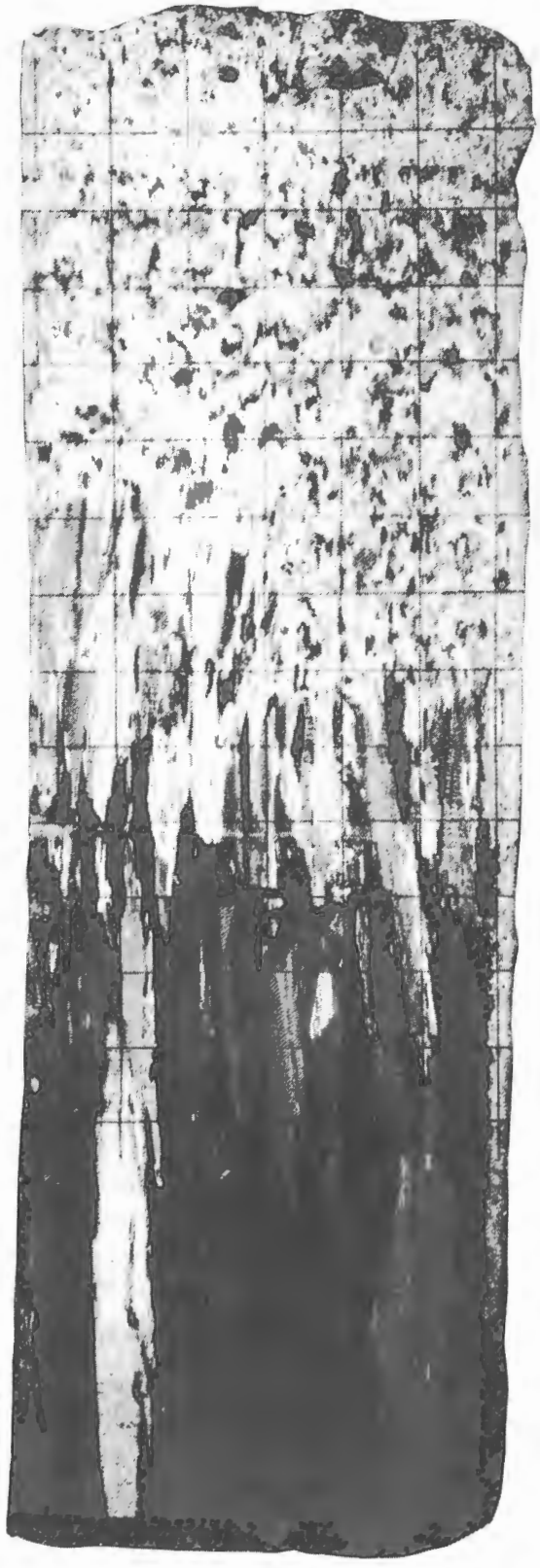

Date : 880310

Station: 10,11 and 12

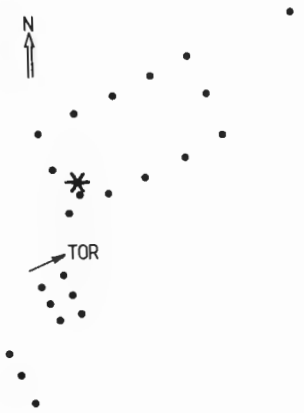

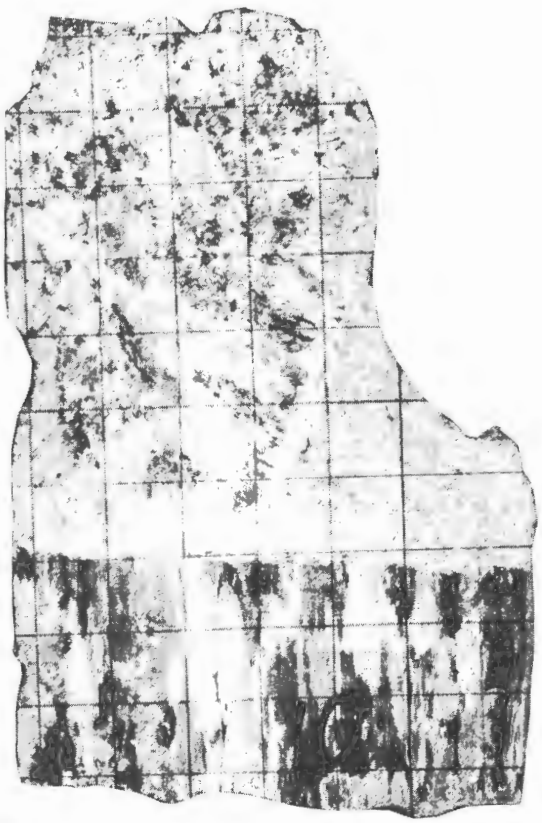

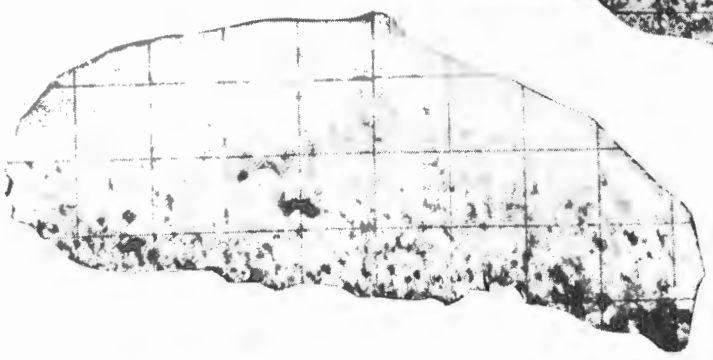

Date : 880310

Station: 20

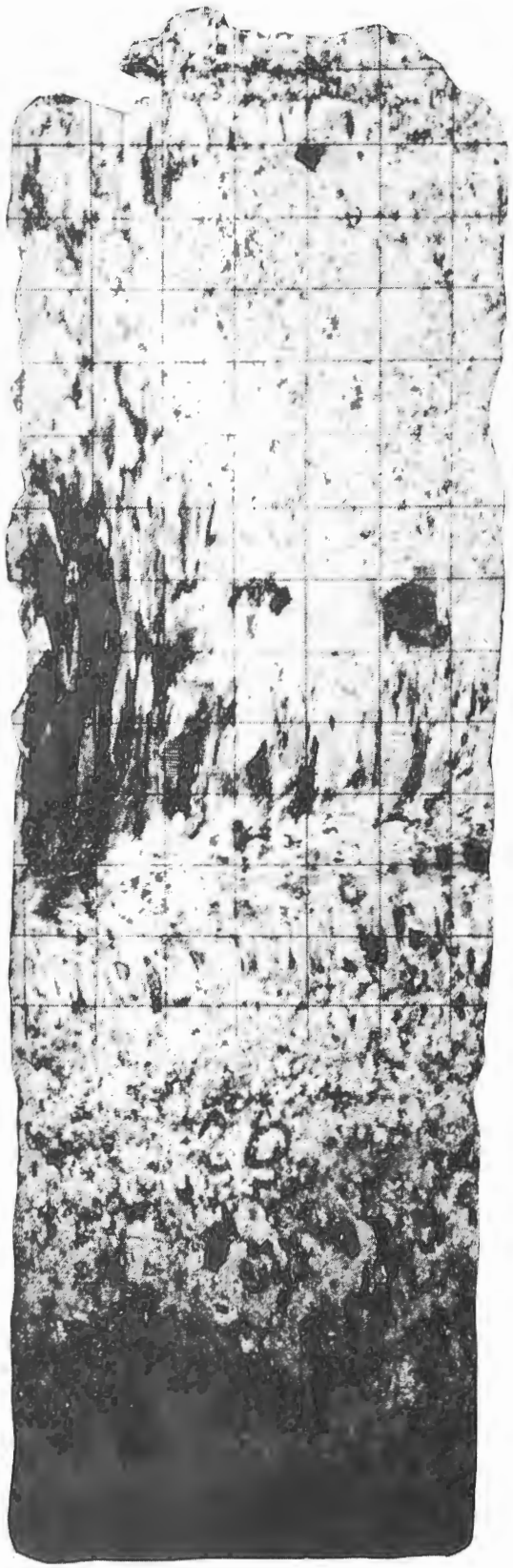

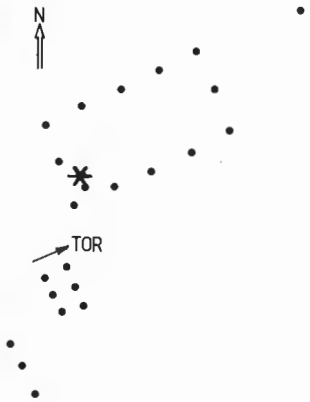

Date : 880310
Station : 23

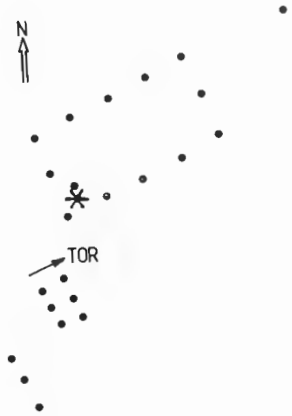

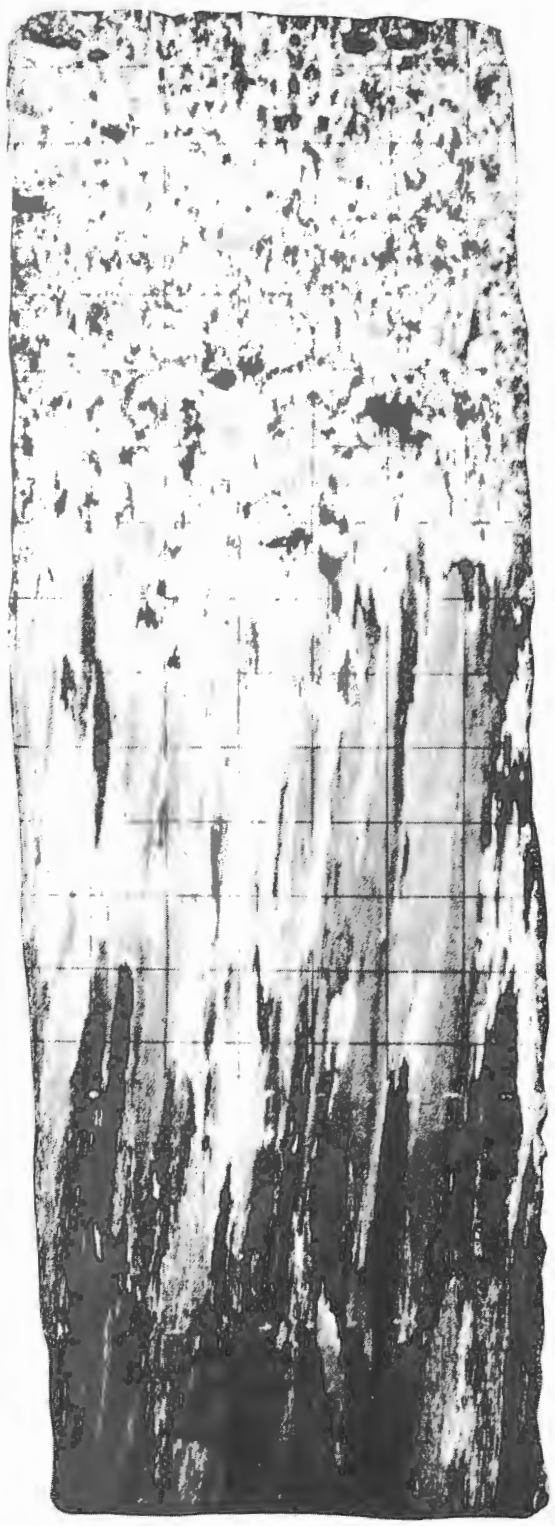

Attachment C

ICE CORE TEMPERATURE, SALINITY, DENSITY, AND POROSITY

ATTACHMENT C

Sea ice core data sampled at TOR during BEPERS-88. Included are also porosity calculations using the method of Schwerdtfeger (1963) (see text). The in situ and laboratory measured ice temperatures are denoted $Temp_i$ and $Temp_l$ respectively.

Station	Datum	Depth (m)	$Temp_i$ (°C)	$Temp_l$ (°C)	Density (kg/m^3)	Salinity (PSU)	Brine	Gas
T1C	880302	5	0.0	0.0	896.7	0.74		
		15	0.0	0.0	916.5	0.50		
		25	0.0	0.0	918.2	0.23		
T2	880302	5	0.0	0.0	904.6	1.62		
		10	0.0	0.0	917.6	0.31		
		25	0.0	0.0	914.3	0.35		
T3	880303	5	-2.4	0.0	902.5	0.83		
		15	-2.2	0.0	903.9	0.67		
		25	-1.6	0.0	884.6	0.46		
		35	0.0	0.0	882.5	0.39		
AB1	880304	5	-3.2	-3.9	868.7	0.93	0.014	0.055
		15	-2.7	-4.1	908.8	0.91	0.017	0.011
		25	-2.2	-4.0	903.1	0.46	0.010	0.017
		35	-1.4	-3.4	916.5	0.73	0.026	0.004
AB3	880304	5	-3.2	-3.0	886.5	1.01	0.015	0.036
		15	-3.0	-3.1	912.4	0.72	0.012	0.007
		25	-2.3	-3.4	916.4	0.33	0.007	0.002
		35	-1.7	-3.3	918.2	0.67	0.020	0.001
AB5	880305	5	-1.6	-2.1	908.1	0.80	0.025	0.013
		15	-1.1	-2.0	910.4	0.39	0.018	0.009
		25	-0.8	-1.7	906.8	0.74	0.046	0.016
		35	-0.6	-1.3	910.3	0.48	0.040	0.011

Station	Datum	Depth (m)	$Temp_i$ (°C)	$Temp_l$ (°C)	Density (kg/m^3)	Salinity (PSU)	Brine	Gas
AB7	880305	5	-2.1	-2.5	907.8	0.90	0.021	0.013
		15	-1.5	-2.5	914.8	0.42	0.014	0.004
		25	-1.2	-2.1	899.0	0.82	0.034	0.023
		35	-0.5	-1.9	911.1	0.63	0.063	0.013
AB9	880309	5	0.0	-3.3	906.4	1.31		
		15	0.0	-3.3	901.7	1.45		
		25	0.0	-3.3	910.1	0.84		
		35	0.0	-3.2	911.2	0.67		
		45	0.0	-3.5	871.2	0.80		
BC3	880309	5	-1.2	-3.6	916.1	0.99	0.042	0.006
		15	-0.2	-3.6	914.6	1.04	0.262	0.027
CD1	880309	5	-1.6	-2.6	909.7	0.66	0.021	0.010
		15	-1.3	-2.9	908.9	0.44	0.017	0.011
		25	-0.7	-3.0	909.3	0.61	0.044	0.013
		35	-0.7	-2.8	914.5	0.30	0.022	0.005
CD3	880309	5	-1.8	-3.2	903.8	1.09	0.030	0.018
		15	-1.1	-3.1	911.5	0.53	0.024	0.009
		25	-0.4	-2.9	916.6	0.49	0.062	0.007
		35	-0.2	-3.0	916.9	0.59	0.149	0.014
CD5	880305	5	-2.6	-1.9	871.9	1.17	0.022	0.052
		15	-2.1	-1.8	915.6	0.43	0.010	0.003
		25	-1.6	-1.9	912.2	0.41	0.013	0.007
		35	-1.0	-2.1	885.3	0.88	0.043	0.039
		45	-0.4	-1.8	776.8	0.99	0.106	0.163
CD7	880305	5	-2.7	-1.8	906.3	0.67	0.012	0.013
		15	-2.5	-1.9	846.6	0.49	0.009	0.078
		25	-2.0	-1.8	915.0	0.52	0.013	0.004
		35	-1.2	-1.9	902.9	0.77	0.032	0.019
		45	-1.2	-1.8	914.1	0.49	0.021	0.006
		55	-0.4	-1.9	864.1	0.96	0.114	0.069

Station	Datum	Depth (m)	$Temp_i$ (°C)	$Temp_l$ (°C)	Density (kg/m^3)	Salinity (PSU)	Brine	Gas
CD9	880305	5	-2.2	-2.2	843.3	1.01	0.021	0.083
		15	-1.8	-2.2	897.0	1.00	0.027	0.025
		25	-0.5	-2.2	911.5	0.29	0.029	0.009
		35	-0.6	-1.3	905.5	0.54	0.045	0.017
DA3	880305	5	-2.4	-2.1	877.0	1.65	0.033	0.048
		15	-1.3	-2.2	910.7	0.71	0.027	0.010
		25	-0.9	-2.1	912.9	0.40	0.022	0.007
		35	-0.5	-1.5	913.1	0.56	0.056	0.010
X	880309	5	0.0	-1.4	911.6	0.64		
		15	0.0	-1.2	908.1	0.74		
		25	0.0	-0.7	915.6	0.37		
S30	880306	5	-1.7	-0.4	868.1	0.80	0.023	0.056
		15	-1.4	-0.9	912.1	0.63	0.023	0.008
		25	-0.8	-1.5	917.7	0.36	0.023	0.002
		35	-0.7	-0.2	917.7	0.66	0.048	0.004
S50	880306	5	-3.1	-1.6	874.4	1.00	0.016	0.049
		15	-2.1	-0.8	912.3	0.43	0.010	0.006
		25	-1.4	-0.6	917.5	0.37	0.013	0.001
		35	-0.7	-0.6	917.5	0.80	0.058	0.005
S70	880306	5	-2.3	-1.9	898.3	0.88	0.019	0.023
		15	-1.8	-1.8	915.0	0.65	0.018	0.004
		25	-1.2	-1.4	916.4	0.30	0.013	0.002
		35	-0.6	-0.9	918.4	0.61	0.051	0.004
T25*	880308	5	-1.3	-2.6	911.4	0.52	0.020	0.008
		15	-1.1	-2.4	909.3	0.88	0.040	0.013
		25	-0.7	-2.7	907.4	0.57	0.041	0.015
		35	-0.6	-2.7	909.6	0.48	0.040	0.012
		45	-0.2	-2.4	890.4	0.56	0.137	0.042

* !UP AND DOWN?

Station	Datum	Depth (m)	$Temp_i$ (°C)	$Temp_l$ (°C)	Density (kg/m^3)	Salinity (PSU)	Brine	Gas
T55	880308	5	-0.6	-2.6	867.5	0.53	0.042	0.058
		15	-0.4	-2.2	900.7	0.37	0.046	0.022
		25	-0.4	-2.4	867.4	0.36	0.043	0.058
		35	-0.4	-2.5	872.3	0.28	0.034	0.052
		45	-0.4	-2.6	853.8	0.28	0.033	0.072
T75	880309	5	-2.6	-2.3	907.6	1.47	0.028	0.014
		15	-1.5	-2.3	914.1	0.55	0.018	0.005
		25	-0.8	-2.1	915.6	0.47	0.030	0.005
		35	-0.2	-2.4	911.2	0.63	0.158	0.021
020	880310	15	0.0	-0.4	873.1	0.39		
		25	0.0	-0.4	904.9	0.52		
		35	0.0	-0.4	840.5	0.47		
		45	0.0	-0.3	854.7	0.44		
021	880310	5	-4.8	-2.0	856.6	0.71	0.007	0.067
		15	-4.9	-2.0	876.6	0.52	0.005	0.045
		25	-4.8	-2.0	752.3	0.31	0.003	0.180
023	880310	5	-2.0	-1.8	844.9	1.00	0.023	0.082
		15	-1.6	-1.4	910.6	0.44	0.014	0.009
		25	-1.0	-1.5	914.1	0.31	0.016	0.005
		35	-0.4	-0.9	918.1	0.78	0.099	0.008

SMHI

Swedish meteorological and hydrological institute
S-60176 Norrköping, Sweden. Tel. +46 11 15 80 00. Telex 64400 smhi s.